

**WAVE ENERGY RESOURCE ASSESSMENT FOR  
SRI LANKA**

Mahanthe Gamage Pravin Maduwantha

198006V

Degree of Master of Science

Department of Civil Engineering

University of Moratuwa

Sri Lanka

July 2020

**WAVE ENERGY RESOURCE ASSESSMENT FOR  
SRI LANKA**

Mahanthe Gamage Pravin Maduwantha

198006V

Thesis submitted in partial fulfilment of the requirements for the degree of Master of  
Science in Civil Engineering

Department of Civil Engineering

University of Moratuwa

Sri Lanka

July 2020

## DECLARATION

I declare that this is my own work and this thesis does not incorporate without acknowledgement any material previously submitted for a Degree or Diploma in any other University or Institute of Higher Learning and to the best of my knowledge and belief it does not contain any material previously published or written by another person except where the acknowledgement is made in the text.

Also, I hereby grant to University of Moratuwa the non-exclusive right to reproduce and distribute my thesis/dissertation, in whole or in part in print, electronic or other medium. I retain the right to use this content in whole or part in future works (such as articles or books).

Signature: .....

Date: .....

The above candidate has carried out research for the MSc Thesis under my supervision.

Name of the supervisor: Dr P. K. C. De Silva

Signature of the supervisor: .....

Date: .....

Name of the supervisor: Mr. A. H. R. Ratnasooriya

Signature of the supervisor: .....

Date: .....

## **ABSTRACT**

Marine energy is recognised as a widely available alternative for energy generated by burning fossil fuels in countries surrounded by seas and oceans. Among the marine energy resources, wave energy contains the highest energy density world-wide. The widespread availability of wave energy resource and relatively low impact of energy intake on the ocean environment have led to numerous research and developments on wave energy harvesting. The direct south-west swell wave approach and relatively narrow continental shelf create more favorable conditions for wave energy harvesting in Sri Lankan coastal region. The assessment of wave energy characteristics in coastal waters of Sri Lanka is important in identifying such a potential.

In this study, ocean waves are projected by a numerical wave model developed using the Simulated Nearshore Wave (SWAN) model, which used atmospheric data obtained by a Global Climate Model (GCM) within two (02) time slices of “present” and “future”. The model output was validated using measured wave data from the southwest coast and other data sources.

The wave output indicates that the coastal areas of Sri Lanka from the southwest to the south-east have a significant amount of wave power. Under the present wave climate, the available wave power varies between 10-30 kW/m. When waves propagate towards the shoreline on the continental shelf, the wave power reduces. Although the southwest monsoon has greatly modulated the offshore wave power up to 30 kW/m, it mostly remains between 10-20 kW/m throughout the year. The spatial variation of wave power along the coast is also obvious. The study also shows that although minor variations are observed, the inter-annual and decadal-scale wave power variation is almost stable.

According to the future wave projections, the average available wave power in the south-west and south-east coastal areas of Sri Lanka will be slightly reduced in the future. This reduction is mainly due to changes in the south-west monsoon system caused by the global climate change. The available wave power resources associated with the swell wave component remain largely unchanged. Although detailed analysis of monthly and annual average wave power shows that strong seasonal and inter-annual changes in wave power can be seen on most of the western and southern coasts of Sri Lanka. Based on the modeled wave outputs of 25-year period, no decadal scale trends can be observed. Finally, the results show that the wave power attributed to sea and swell waves very stable over the long term with a slight wave power reduction in the future.

**Keywords:** Wave power, Wave projections, Climate change, Monsoons, Sri Lanka, Indian Ocean

## **ACKNOWLEDGEMENT**

I would like to express my sincere gratitude to my supervisor Dr. P. K. C. De Silva for his immense support, guidance and encouragement throughout this research. Because of his support I was able to successfully complete my masters and also able to get a very big exposure to local and international environments. And also I would like to express my sincere gratitude to my co-supervisor Mr. Harsha Ratnasooriya for his immense support and guidance for the successful completion of my masters.

Also I should acknowledge Prof Harshani for initiating the study, providing financial assistance and also the technical guidance and encouragement. Dr Bahareh should be acknowledge for carrying out large scale modelling and providing the data used for the study without which this research would not have been possible.

Further, I would like to express my appreciation to the Research Coordinator of the Department of Civil Engineering, University of Moratuwa, Dr. J. C. P. H. Gamage, who instructed me to improve my research work. And also I would like to express my gratitude to Prof. S.A.S. Kulathilaka, Head of Department, Department of Civil Engineering for the support extended.

My special thanks go to the Swansea University for providing the financial support through the Global Challenge Research Fund project 'Wave energy resource characterization for Sri Lanka in a changing ocean climate' to carry out this research study. The Japan Meteorological Agency is acknowledged with gratitude for sharing atmospheric model outputs to run the wave models.

## TABLE OF CONTENTS

DECLARATION .....	ii
ABSTRACT .....	iii
ACKNOWLEDGEMENT .....	iv
TABLE OF CONTENTS .....	v
LIST OF FIGURES .....	vii
LIST OF TABLES .....	<b>Error! Bookmark not defined.</b>
LIST OF ABBREVIATIONS .....	xii
1.0 INTRODUCTION .....	1
1.1 Background .....	1
1.2 Problem Statement .....	1
1.3 Study Area .....	2
1.4 Research Objectives .....	4
1.6 Structure of the Thesis .....	4
2.1 Introduction .....	5
2.2 Origins of Wave Power and its Global Distribution .....	5
2.3 Wave power estimation .....	6
2.4.1 Measured data set at Galle .....	9
2.4.1 Measured wave data set at Matara .....	12
2.5 Regional-scale wave energy assessments .....	18
2.5.1 Mediterranean Sea .....	18
2.5.2 Southern Caspian Sea .....	18
2.5.3 Peninsular Malaysia .....	19
2.5.4 Canary Islands .....	19
2.5.5 Shandong peninsula, China .....	21
2.5.6 Other similar studies on wave energy potential .....	22
2.6 Wave energy assessments for Sri Lankan region .....	23
2.7 Impact of global climate change on wave energy resource .....	24
3.0 RESEARCH METHODOLOGY .....	26
3.1 Introduction .....	26
3.2 Methodology flow chart .....	26
4.0 WAVE MODEL AND MODEL VALIDATION .....	27

4.1 Introduction .....	27
4.2 Process of the development of the wave model .....	27
4.3 Model validation.....	29
<b>5.0 EVALUATION OF SPATIO-TEMPORAL VARIABILITY OF WAVE ENERGY RESOURCE .....</b>	<b>36</b>
5.1 Introduction .....	36
5.2 Wave power distribution around Sri Lanka.....	36
5.2.1 Spatial distribution of wave power .....	36
5.2.2 Temporal and directional variations at selected sites.....	39
5.2.3 Wave power matrix .....	46
5.2.4 A summary of available wave energy resource .....	51
<b>6.0 IMPACTS OF GLOBAL CLIMATE CHANGE ON THE OCEAN WAVE ENERGY RESOURCE.....</b>	<b>53</b>
6.1 Introduction .....	53
6.2 Climate change impact on wave power variations .....	53
6.2.1 Spatial distribution of future wave power.....	54
6.2.2 Effect of monsoon systems .....	57
6.2.3 Temporal and directional wave power variations in the future.....	59
6.2.4 Changes in power fraction .....	65
<b>7.0 CONCLUSIONS.....</b>	<b>69</b>
7.1 Introduction .....	69
7.2 Wave power potential.....	69
7.3 Temporal variations of wave power .....	70
7.2 Climate change impact on wave energy resource .....	70
<b>REFERENCES.....</b>	<b>72</b>

## LIST OF FIGURES

Figure 1.1: Location of Sri Lanka in the Indian Ocean.....	2
Figure 1.2: Sea Bed Bathymetry Map of the Coastal Regions of Sri Lanka. (The contour heights are given in) meters).....	3
Figure 2.1: Global distribution of annual mean wave power (Source: (Cornett, 2008)).....	6
Figure 2.2: A simple sinusoidal wave (source: (World Meteorological Organization, 1998) .....	7
Figure 2.3: Buoy locations of measured data sets.....	9
Figure 2.4: A sample of measured time series of offshore sea/swell significant wave height (a) and period (b).....	10
Figure 2.5: Significant swell wave height roses determine from waves measured off the south-west coast of Sri Lanka in Galle over a period of 3 years between 1989 and 1992.....	11
Figure 2.6: Location of Matara Buoy 1 (Source: Google Earth).....	12
Figure 2.7: Location of Matara Buoy 2 (Source: Google Earth).....	12
Figure 2.8: Time series of measured significant wave height $H_s$ (a) and period $T$ (b) time series of Matara B1 (red) and B2 (blue) .....	14
Figure 2.9: Significant wave height roses determine from waves measured at Matara wave boy 2 during April 2013 – April 2014.....	15
Figure 2.10: The annual mean spatial distribution of wave energy around Malayasia (Source: (Mirzaei A., Tangang F, Juneng L., 2016) .....	20
Figure 2.11: Average annual wave power along the Canary Islands (Source: (Gonçalves M., Martinho P., Soares C.G., 2014) .....	21
Figure 2.12: Distribution of average wave energy density (kW/m) in Shandong-China (Source: (Liang B., Fan F., Yin Z., Shi H., Lee D., 2013).....	22
Figure 3.1: Research methodology flow chart .....	26



Figure 4.1: (a) Indian Ocean KU_IO, (b) KU_IND and (c) KU_SLK wave model domains used to generate wave projections for the Sri Lanka region.....	28
Figure 4.2: Map with all data locations used for wave model validation. GMO – Galle (Modelled), GE - Galle (ERA-Interim), GM - Galle (Measured), P1 and P2 are additional model validation points .....	31
Figure 4.3: Comparison of modelled [at GMO, (5.93° N 80.23° E)] (green), ERA-Interim Reanalysis [at GE (6.0N, 80.250E) (yellow) and measured [at GM (5.93 N, 80.23E)] (red) wave height time series .....	31
Figure 4.4: Comparison of modelled [at GMO, (5.93° N 80.23° E)] (green), ERA-Interim Reanalysis [at GE (6.0N, 80.250E) (yellow) and measured [at GM (5.93 N, 80.23E)] (red) monthly average significant wave heights .....	32
Figure 4.5: Comparison of modelled [at GMO, (5.93° N 80.23° E)] (green), ERA-Interim Reanalysis [at GE (6.0N, 80.250E) (yellow) and measured [at GM (5.93 N, 80.23E)] (red) monthly average wave period .....	32
Figure 4.6: A comparison of ERA-Interim data and modelled significant wave heights during the period 1999-2003 at points P1 and P2.....	33
Figure 4.7: A comparison of modelled and ERA-Interim Reanalysis mean energy period during the period 1999-2003 at points P1 and P2.....	34
Figure 4.8: A comparison of modelled (green) and ERA-Interim Reanalysis (yellow) monthly averaged significant wave height and mean energy period during the period 1999 and 2003 at points P1 (top) and P2 (bottom) .....	35
Figure 5.1: A spatial distribution of average wave power (averaged over the simulated 25-year period between 1979 and 2003) for the Sri Lankan domain.....	37
Figure 5.2: Spatial distribution of monthly average wave power (averaged over the modelled 25-year period between 1979-2003) for the entire coastline of Sri Lanka.	38
Figure 5.3: Eighteen nearshore (PN-1 to PN-9) and offshore (PO-1 to PO-9) locations selected along the south-west to south-east coast of Sri Lanka for detailed wave resource analysis. ....	39

Figure 5.4: Wave power distribution at the selected nearshore locations (PN-1 to PN-9) around the south-west to south-east coastline of Sri Lanka. ....	41
Figure 5.5: Wave power distribution at the selected offshore locations (PO-1 to PO-9) around the south-west to south-east coastline of Sri Lanka. ....	42
Figure 5.6: Box-Whisker plots of offshore and nearshore wave power around the south-west to south-east coastline of Sri Lanka.(for PN-01 to PN-05). ....	43
Figure 5.7: Box-Whisker plots of offshore and nearshore wave power around the south-west to south-east coastline of Sri Lanka.(for PN-06 to PN-09). ....	44
Figure 5.8: Annual average wave power os selected 18 locations for the period 1979-2003. Broken lines refer to the nearshore points while dark lines refer to the offshore points .....	46
Figure 5.9: Power matrices of available wave power at locations PN-1 to PN-5. Power is given as a fraction of available power in each sea state to total power available at the selected location .....	48
Figure 5.10: Power matrices of available wave power at locations PN-6 to PN-9. Power is given as a fraction of available power in each sea state to total power available at the selected location .....	49
Figure 5.11: Power matrices of available wave power at locations PO-1 to PO-5. Power is given as a fraction of available power in each sea state to total power available at the selected location .....	50
Figure 5.12: Power matrices of available wave power at locations PO-6 to PO-9. Power is given as a fraction of available power in each sea state to total power available at the selected location .....	51
Figure 5.13: A summary of spatial variation and range of variation of wave power around south-west to south-east coast of Sri Lanka. The radius of circles proportional to the amount of average wave power. Red, yellow and green in the colour bar indicates high, average and low range of variability of wave power. ....	52

Figure 6.1: The distribution of average wave power around Sri Lanka. (a) ‘present’ 25-year simulation period from 1979 to 2003 ; and (b) ‘future’ 25-year simulation period from 2075 to 2099.....	54
Figure 6.2: The distribution of difference between ‘future’ and ‘present’ average wave power (Future-Present) around Sri Lanka.....	55
Figure 6.3: The difference between ‘future’ and ‘present’ monthly averaged wave power.....	56
Figure 6.4: Difference between ‘future’ and ‘present’ average wave power during (a) monsoon (May-September) and (b) non-SW-monsoon (October-April) periods.....	57
Figure 6.5: Difference between ‘future’ and ‘present’ average significant wave height during (a) monsoon (May-September) and (b) non-SW-monsoon (October-April) periods.....	58
Figure 6.6: Difference between ‘future’ and ‘present’ average Tm-10 during (a) monsoon (May-September) and (b) non-SW-monsoon (October-April).....	58
Figure 6.7: Offshore locations around the west and south coast selected.....	59
Figure 6.8: Present and future annual average wave power around Sri Lanka for M1 to M10. X-axis gives the year number, starting from the beginning of the ‘present’ and ‘future’ 25-year simulation time slices. ....	61
Figure 6.7: Box-Whisker diagrams of current and future wave power resource at locations M1 to M10. ....	63
Figure 6.9: Wave power roses representing ‘present’ wave climate .....	64
Figure 6.10: Wave power roses representing ‘future’ wave climate .....	65
Figure 6.11: Variation of available wave power at different energy period and significant wave height classes as a fraction of total available power (for sea waves) .....	66
Figure 6.12: Variation of available wave power at different energy period and significant wave height classes as a fraction of total available power (for swell waves) .....	67

## **LIST OF TABLES**

Table 4.1: Details of all data locations used for wave model validation.....	30
Table 6.1: Coordinates and water depths of locations selected for detailed analysis of climate change impacts on the wave resource around Sri Lanka .....	60

## **LIST OF ABBREVIATIONS**

<u>Abbreviation</u>	<u>Description</u>
AGCM	Atmospheric Global Climate Model
GCM	Global Climate Model
GMO	Galle Modelled data
GE	Galle ERA-Interim data
GM	Galle Measured Data
IOD	Indian Ocean Dipole
NAO	North Atlantic Oscillation
RMSE	Root Mean Square Error
SO	Southern Oscillation
SWL	Still Water Level

# **1.0 INTRODUCTION**

## **1.1 Background**

Significant environmental implications associated with energy production using non-green sources and ever increasing global energy demand have led investigations into exploring the potential to generate energy from renewable resources. Among numerous forms of renewable energy sources, ocean wave energy has been recognised as having one of the highest energy densities worldwide (Kamranzad B., Shahidi A. E., Chegini V., 2016). In addition, low environmental implications and minimal or no use of land have made wave energy an option favored by many countries (Iglesias G., Lopez M., Carballo R., Castro A., and Fraguera J.A. , 2009). As a result, numerous countries bordering oceans have conducted studies to assess and quantify available wave energy resource, which is the primary requirement for planning and implementation of wave energy harvesting projects.

## **1.2 Problem Statement**

The electricity demand in Sri Lanka is growing at a rate of 6 % per year and which requires importing large quantities of fossil fuels-coal and petroleum-to meet the needs of current electricity generation methods. In view of the high cost of such imports and the adverse environmental impacts associated with such methods, it is important to examine the potential of extracting energy via renewable sources. Ocean wave energy is being increasingly regarded as a promising renewable energy resource. Because of the exposure of the coast of Sri Lanka to the waves generated in the Indian Ocean, a high potential exists to harness the wave energy as a sustainable source. However, no detailed assessment of wave energy potential in the ocean around Sri Lanka has been carried out and a strong need exists for such an assessment in order to develop wave energy as a sustainable energy source in the country. This ~~thesis~~ study attempts to address this knowledge gap by establishing a detailed wave energy resource assessment for Sri Lanka.

### 1.3 Study Area

Sri Lanka is located in the northern Indian Ocean between 5°-10° N latitude, north of the equator and between 79°-82° E longitude (Figure 1.1). The country receives energetic swell waves approaching from the south, thus making it an ideal location for ocean wave energy harvesting. As a member of the Global Vulnerability Forum, Sri Lanka is currently exploring renewable alternatives for its heavy fossil fuel dependent energy generation. The Sri Lankan Government has identified ocean wave energy as one of the six (06) green energy alternatives which are to be explored further as potential future renewable energy developments.

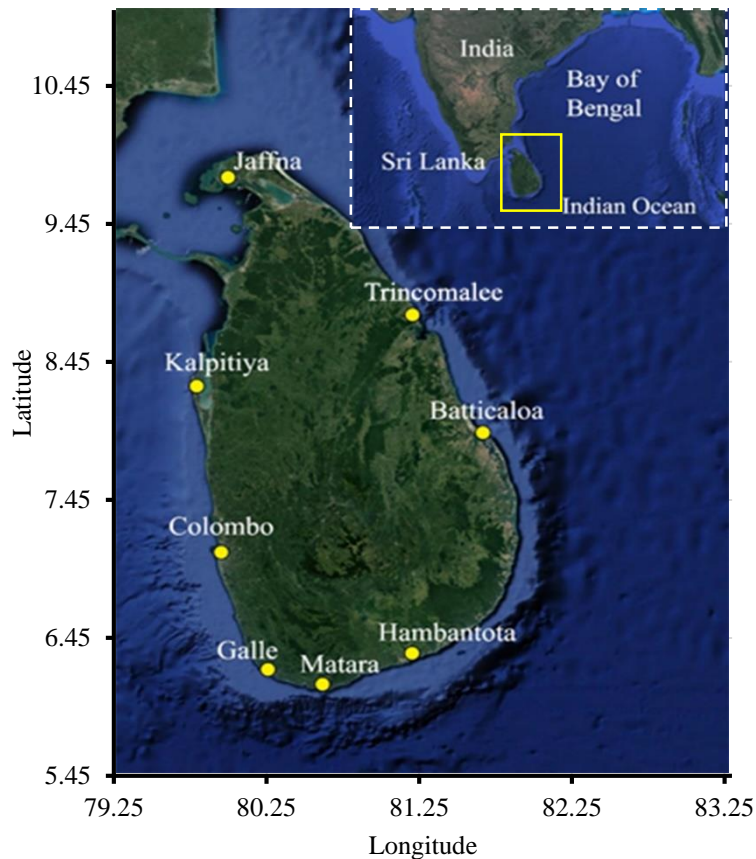


Figure 1.1: Location of Sri Lanka in the Indian Ocean

Sri Lanka is surrounded by a narrow continental shelf of width varying between 5 km and 25 km, which separates the island from the Indian sub-continent (Figure 1.2). The water depth at the margin of the shelf varies between 50m to 200 m. The narrowest

part of the shelf is located off the coast of Matara on the south coast. The water depth beyond the edge of the shelf sharply increases to more than 1000 m within a very short distance. Long-distance swell waves generated in the Southern Indian Ocean directly approaches the western and southern shores of Sri Lanka all year round. The swell wave approach direction is found to be predominantly south. The swell waves are superimposed and modulated by the highly energetic south-westerly wind waves generated during the south-west tropical monsoon that operates in the Northern Indian Ocean between May and September. The north-east tropical monsoon, which falls between December and February, generates high sea waves in the northern and eastern coastal regions (Department, 1997).

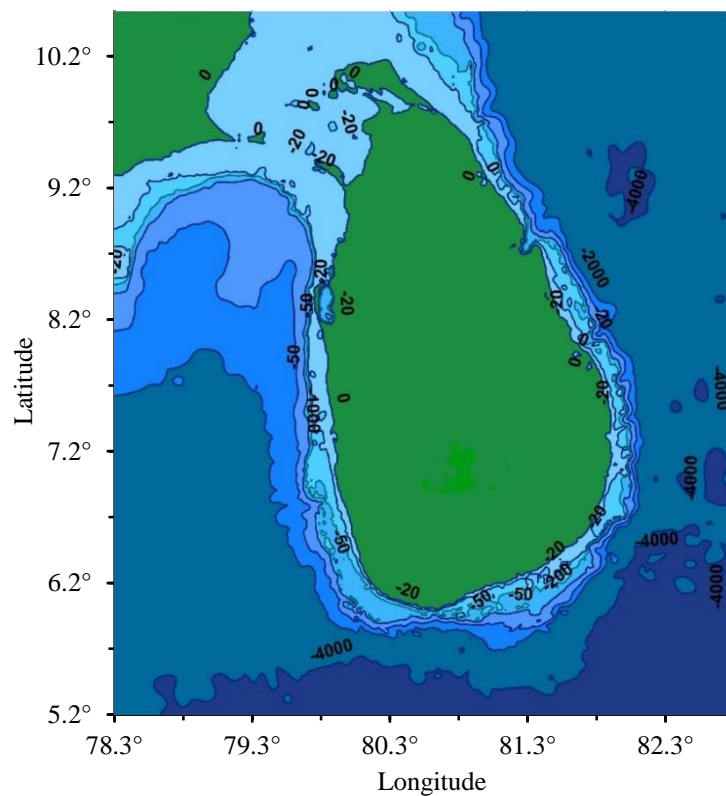


Figure 1.2: Sea Bed Bathymetry Map of the Coastal Regions of Sri Lanka. (The contour heights are given in)

It has been found, based on the measured set of wave data off the coast of Galle (at 70m depth), that on average the significant swell wave heights in the south and west



coasts of Sri Lanka vary between 0.5 m and 2.5 m while that of sea waves vary between 0.2 m and 3.0 m. Sea waves have found to have wave periods averaged around 4 s while swell waves have periods around 11 s (Sheffer H.J., Fernando K.R.M.D., Fittschen T., 1994). The 05, 50 and 100-year return period significant sea wave heights during the south-west monsoon are found to be 4.12 m, 5.22 m and 5.58 m respectively and that of swell waves are 2.82 m, 3.00 m and 3.03 m respectively (Thevasiyani T., Perera K., 2014).

#### **1.4 Research Objectives**

The main aim of this research is to assess the ocean wave energy potential around Sri Lanka. To achieve this objective, four (04) specific objectives have been defined:

- To evaluate the spatial distribution of wave energy resource along the south coast of Sri Lanka to identify the wave energy hotspots
- To estimate the temporal variation of wave energy resource over a range of timescales to evaluate its stability and sustainability
- To analyze the variation of wave energy at nearshore and offshore regions
- To evaluate the temporal and spatial variations of wave energy resource in changing climate conditions around Sri Lanka

#### **1.6 Structure of the Thesis**

This Thesis includes seven (7) chapters, including the introductory chapter. Chapter 1 presents briefly the background, problem statement, research objectives of the study. Chapter 2 focuses on defining the wave power, relevant studies carried out earlier and the importance of assessing climate change impact on wave energy resource. Chapter 3 describes the research methodology. The development of the wave model is presented in chapter 4. The chapter 5 includes the analysis on available wave power and the chapter 6 assesses the climate change impacts on wave energy resource around Sri Lanka. Chapter 7 presents the conclusions of the study.

## 2.0 LITERATURE REVIEW

### 2.1 Introduction

The literature review is presented in 05 parts. The first part focuses on identifying wave energy and the second part focuses on wave power equation and basic concepts on wave power quantification. The third part presents details on available wave measurements in Sri Lanka and the wave climate based on such measurements. The next part focusses on a few similar studies carried out in other parts of the world to assess the wave energy resource. The last part includes the details on assessing global climate change impacts on wave energy resource.

### 2.2 Origins of Wave Power and its Global Distribution

Wave energy can be considered as an indirect result of solar radiation and modulated by the wind field associated with the ocean water surface. Basically, winds are generated due to differential heating (uneven heating) of the earth's atmosphere. When wind blows over a vast stretch of water surface, a part of its energy is converted to water waves (Thomas J., Barve K.H., Dwarakish G S., Ranganath L. R., 2015). The amount of transmitted energy depends on;

- 1) Wind speed
- 2) The length of the time period
- 3) The 'Fetch' (distance over which wind blows)

When the ocean waves are within the wave generation area, they are known as 'Sea waves'. The ocean waves can travel out of the storm area if there is an adequate water depth with a minimal energy loss. These types of waves are known as 'Swell waves' which can travel for thousands of kilometers becoming regular and smooth waves. Swell waves are much more consistent and reliable when considering wave energy harvesting. Being an island in the Indian Ocean, west and south coasts of Sri Lanka have the advantage of receiving long-distance direct swell waves. Even though a significant progress can be seen in research studies, testing and designs towards wave energy harvesting, still in an immature phase when compared to wind and solar energy sectors.

Recent studies reveal that the global offshore wave energy potential is about 10TW which is capable of satisfying the entire global energy demand (Kamranzad B., Shahidi A. E., Chegini V., 2016). Cornett (2008) carried out a broad-scale study on global wave resource using numerically simulated ocean waves. He presented a range of parameters including ‘energy period’, that can be used to describe and quantify the temporal variation of wave energy resource at a given location. He also highlighted the importance of considering the frequency and intensity of extreme wave conditions when evaluating wave energy resource. His study has also been useful to identify regions which have the highest wave energy potential in the world (Figure 2.1).

According to Figure 2.1, the most energetic seas with annual mean wave power between 50 to 70 kW/m or higher, can be observed near 30° and 60° latitudes where strong storms occur. However, the lower power levels may be more preferable to wave energy harvesting when they have a low temporal variability

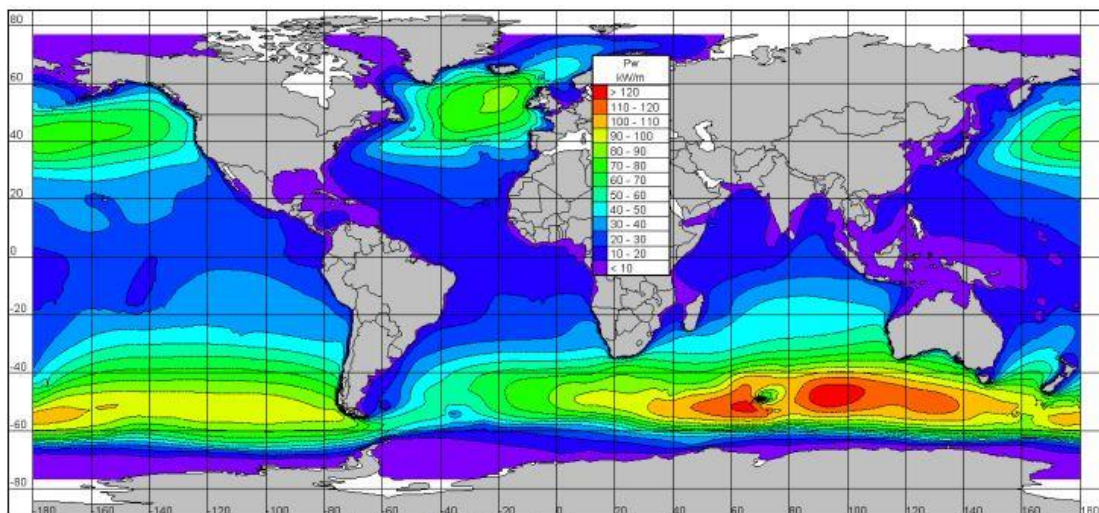


Figure 2.1: Global distribution of annual mean wave power (Source: (Cornett, 2008))

### 2.3 Wave power estimation

In this study most of the covered area by the model domain can be considered as deep sea areas. The equations generated based on linear wave theory are sufficiently accurate estimating wave parameters in deep sea. The concept of Linear Wave Theory describes ocean wave as a simple sinusoidal or cosine wave.

The point at the maximum elevation over the still water level (SWL) is called the wave crest and the lowest point below the SWL is called the trough (refer to Figure 2.2). The wave height ( $H$ ) is defined as the total distance from crest to the trough. The amplitude ( $a$ ) is defined as the distance between the SWL and crest or SWL and trough. The wave length ( $L$ ) of a regular sinusoidal wave is defined as the horizontal distance between successive points of equal amplitude and phase (World Meteorological Organization, 1998).

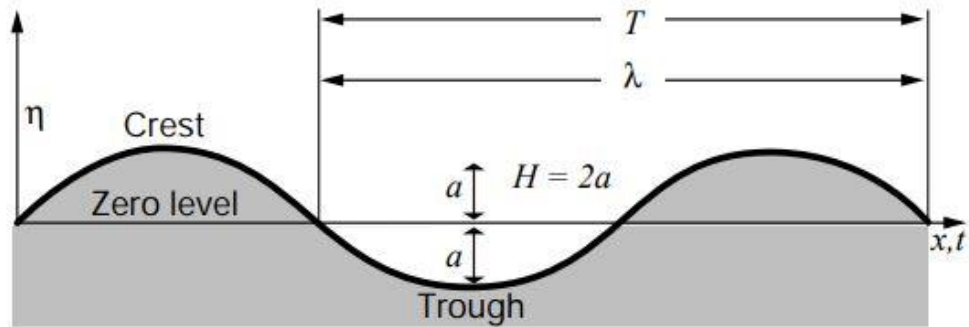


Figure 2.2: A simple sinusoidal wave (source: (World Meteorological Organization, 1998)

Considering a simple sinusoidal wave, the free surface elevation can be calculated as in the Equation (1) as a function of time ( $t$ ),

$$\eta = \frac{H}{2} \cos\left(\frac{2\pi x}{\lambda} - \frac{2\pi t}{T}\right) \quad (1)$$

Where;

$\eta$  = free surface elevation

$H$  = wave height

$x$  = horizontal distance (in the direction of  $x$ )

$\lambda$  = wave length

$t$  = time

$T$  = wave period

The total energy of a wave system is the sum of its potential energy and kinetic energy. The standard form of measurement of ocean wave power is kilowatts (kW) per meter

of wave crest length. The energy flux or power ( $P$ ) transmitted by a regular wave per unit crest width can be written as;

$$P = \frac{1}{8} \rho g H^2 C_g \quad (2)$$

Where;

$P$  = power transmitted per unit crest width

$\rho$  = density of the fluid

$g$  = gravitational acceleration

$H$  = wave height

$C_g$  = group velocity

The group velocity ( $C_g$ ) can be defined as;

$$C_g = \frac{1}{2} \left( 1 + \frac{2kh}{\sinh 2kh} \right) \frac{\lambda}{T} \quad (3)$$

Where;

$h$  = local water depth

$k$  = wave number ( $k = 2\pi/L$ )

## 2.4 Measured wave data in Sri Lanka

### 2.4.1 Measured data set at Galle

Some wave measurements have been reported at two locations around Sri Lanka. Coast Conservation and Coastal Resources Department of Sri Lanka (CCD), with the corporation of the German Agency for Technical Corporation (GTZ) has carried out a continuous wave measurement program off the coast of Galle (Figure 2.3), at a water depth of 70m, over a period of 3.5 years between 1989 and 1992 (Sheffer H.J., Fernando K.R.M.D., Fittschen T., 1994). Waves were measured using a DATAWELL B.V. directional wave buoy for 30 mins duration every three hours. Waves at the measurement location are assumed to be representative of the wave climate in the south-west of Sri Lanka. Those measurements concluded that long-distance swell waves occupied a significant proportion of wave energy spectrum.

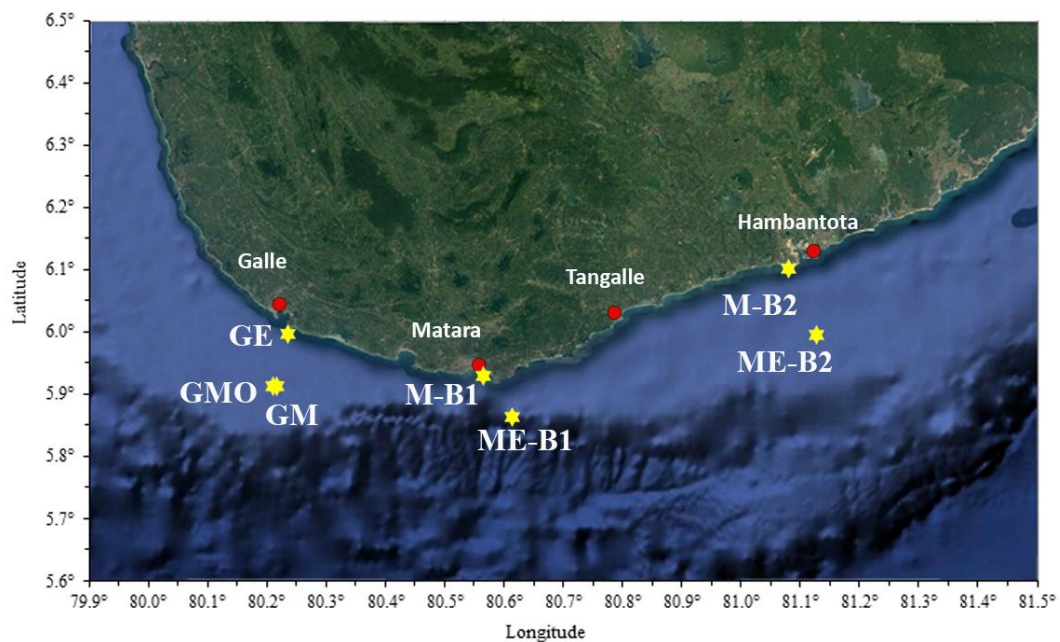


Figure 2.3 Buoy locations of measured data sets

A sample measurement of sea and swell wave conditions is given in Figure 2.4. The figure shows a clear seasonal variability of sea waves where highly energetic seas prevail during the south-west monsoon between May and September.

The magnitude of significant swell wave heights varies between 0.5m to 2.5 m while that of sea waves varies from 0.2m to 3.0 m during the measurement period. On average, sea waves have wave periods around 4 s while swell waves have periods around 11 sec. Swell wave roses determined from the measurements (Figure 2.5) show that the predominant swell wave approach direction is south. The wave measurement procedure and a detailed analysis of the wave climate of the south-west of Sri Lanka can be found in Sheffer et al. (1994).

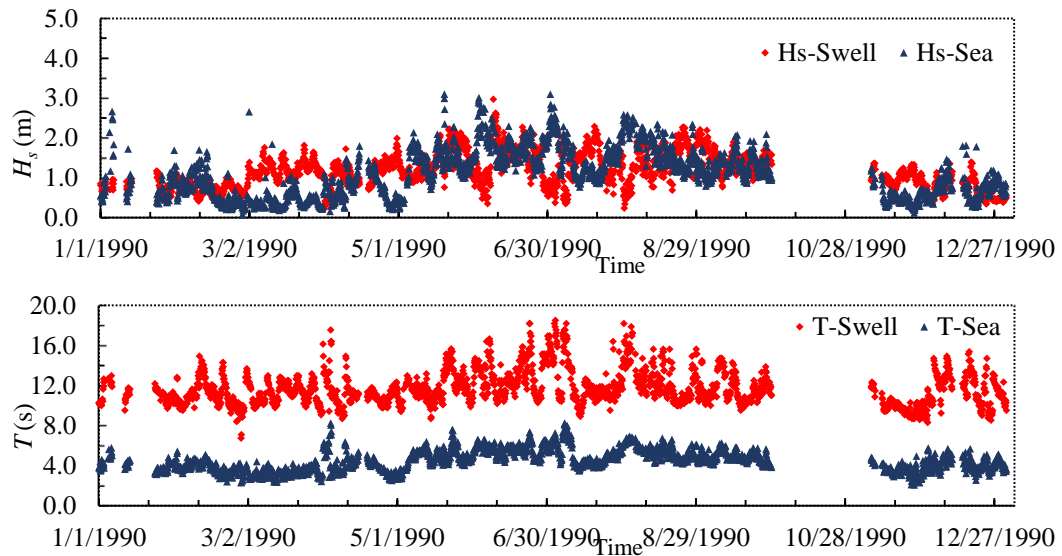


Figure 2.4: A sample of measured time series of offshore sea/swell significant wave height (a) and period (b)

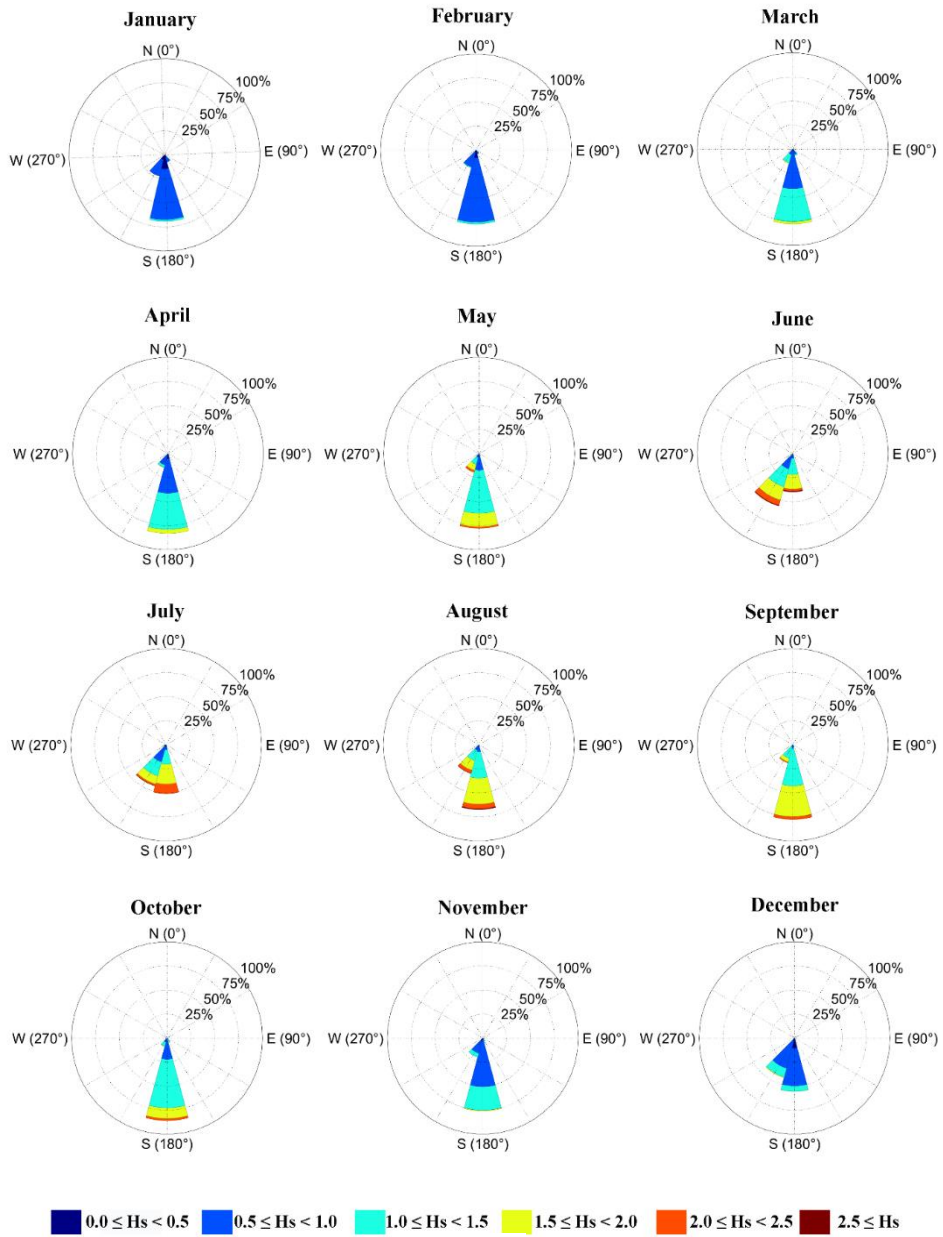


Figure 2.5: Significant swell wave height roses determine from waves measured off the south-west coast of Sri Lanka in Galle over a period of 3 years between 1989 and 1992



#### 2.4.1 Measured wave data set at Matara

Recently, wave measurements have been carried out at two locations off the coast of Matara, located in the south coast of Sri Lanka (Figure 2.6 and Figure 2.7) at 20 m (non-directional Buoy 1) and 10 m (Buoy 2) water depths (<http://www.sciencedb.cn/dataSet/handle/447>). The measurements contain wave time series (significant wave height and corresponding wave period) at the two water depths for a period of five months (Sept. 2013 – Feb. 2014) at Buoy 1 and of one year (April 2013 – April 2014) at Buoy 2.



Figure 2.6: Location of Matara Buoy 1 (Source: Google Earth)



Figure 2.7: Location of Matara Buoy 2 (Source: Google Earth)

Concurrent wind records have also been collected at an automated weather station at a nearby seaside land point. Measured wave conditions are shown in Figure 2.8. Those data have been used to determine the monthly percentage of sea and swell wave conditions and has found that swell wave component is greater than 57% all throughout the year and reached 77% in November 2013 (Luo et al., 2018). A seasonal signal similar to Galle measured data (Figure 2.4) can be seen where south-west monsoon between May and September brings larger waves to the south coast. The average significant wave height during the south-west monsoon is 1.5 m while that outside monsoon period is around 1.0 m. The average wave period is around 9.0 s. Wave height roses for Matara Buoy 2 data are shown in Figure 2.9. The predominant wave approach direction has been identified as the south, except from December to March where a significant proportion of waves approach from the south-east. It should be noted that considerable local effects can be expected on wave height and direction at measured at buoy 2, which is located in shallow 10 water depth. A detailed description of the measurement programme, results and analysis can be found in Luo et al. (2018).

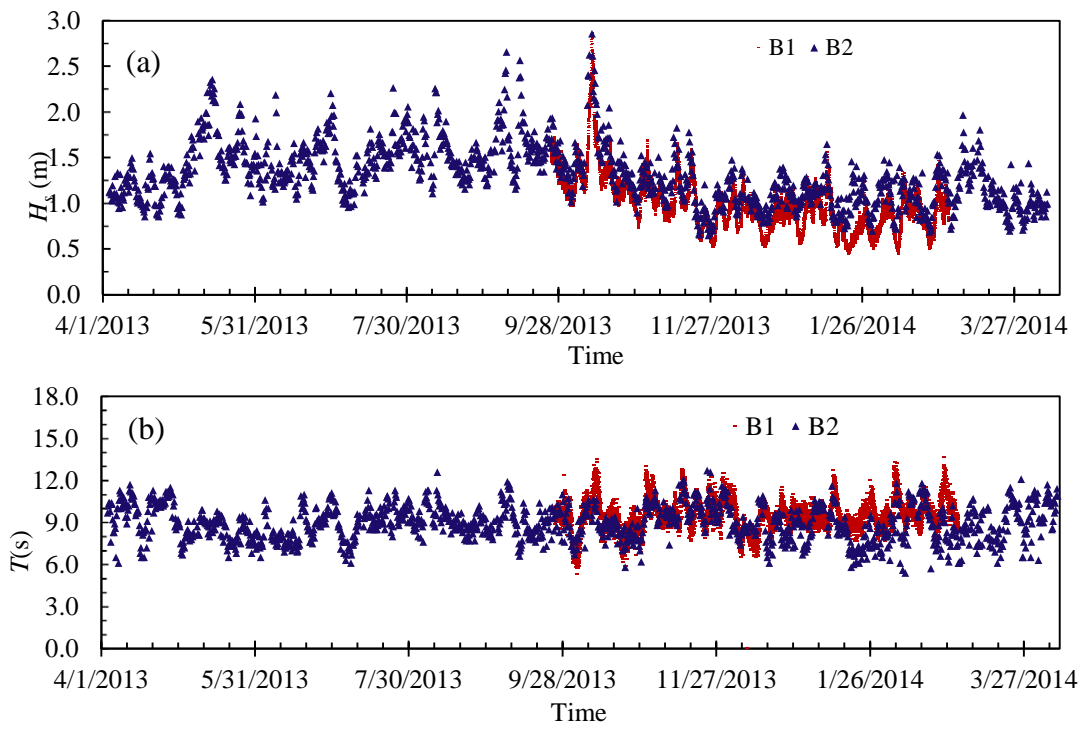


Figure 2.8: Time series of measured significant wave height  $H_s$  (a) and period  $T$  (b) time series of Matara B1 (red) and B2 (blue)

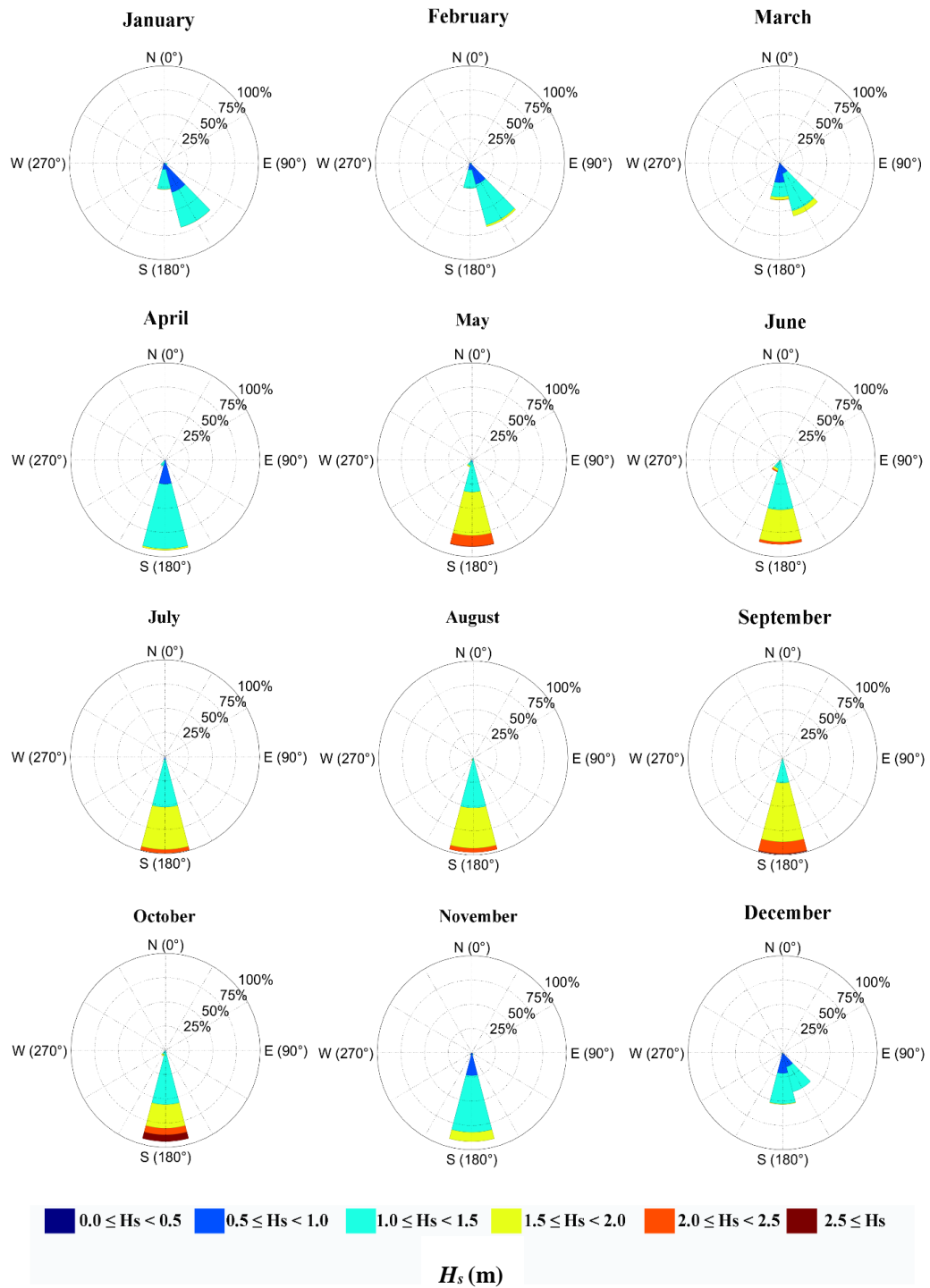


Figure 2.9: Significant wave height roses determine from waves measured at Matara wave boy 2 during April 2013 – April 2014

According to the dispersion equation, the relation between wave length, depth and wave period can be described as (Equation 4),

$$L = T \sqrt{\frac{g}{k} \tanh(kh)} \quad (4)$$

Where;

$L$  = wave length

$g$  = gravitational acceleration

$h$  = local water depth

$T$  = wave period

$k$  = wave number ( $k = 2\pi/L$ )

In shallow water ( $h < L/2$ ), the Equation (5) can be used without noticeable error to calculate the wave length ( $L$ ).

$$L = \frac{gT^2}{2\pi} \left\{ \tanh \left[ \left( \frac{4\pi h}{gT^2} \right)^{3/4} \right] \right\}^{2/3} \quad (5)$$

But in deep water ( $h > L/2$ ), following simplifications can be made,

$$C = \frac{L}{T} = 2C_g \quad \text{and} \quad L = L_0 = \frac{gT^2}{2\pi}$$

Therefore, the power transmitted per unit crest width in deep water ( $P_0$ ) can be defined as,

$$P_0 = \frac{1}{32\pi} \rho g^2 H^2 T \quad (6)$$

Where;

$P_0$  = power transmitted per unit crest width

But the real sea state is consisting with large number of regular waves with different directions, wave heights, amplitudes and frequencies. This mix of wave parameters often described by a two-dimensional (2D) wave spectrum  $S(f, \theta)$  or variance spectral density function where  $f$  and  $\theta$  are wave frequency ( $=2\pi/T$ ) and wave

direction. Considering the spectral density, the power transmitted per unit width can be expressed as;

$$P = \rho g \int_0^{2\pi} \int_0^{\infty} C_g(f, h) S(f, \theta) df d\theta \quad (7)$$

With,

$$C_g(f, h) = \frac{1}{2} \left[ 1 + \frac{2kh}{\sinh 2kh} \right] \sqrt{\frac{g}{k} \tanh(kh)} \quad (8)$$

Where;

$k(f)$  = frequency dependent wave number

Considering irregular waves, the wave power transmitted can be approximated introducing the energy period ( $T_e$ ) as follows,

$$P \approx \frac{1}{16} \rho g H_s^2 C_g(T_e, h) \quad (9)$$

Where;

$H_s$  = significant wave height

$C_g(T_e, h)$  = group velocity of a wave with period  $T_e$  at water depth  $h$

The  $T_e$  of a random sea state is defined in terms of the zeroth ( $m_0$ ) and the first negative ( $m_{-1}$ ) spectral moments as,

$$T_e = \frac{m_{-1}}{m_0} = \frac{\int_0^{2\pi} \int_0^{\infty} f^{-1} S(f) df d\theta}{\int_0^{2\pi} \int_0^{\infty} S(f) df d\theta} \quad (10)$$

The water depth is greater than the half of wave length in deep water ( $h > L/2$ ). Therefore, the transmitted wave power per unit width simplifies to,

$$P \approx \frac{1}{64\pi} \rho g^2 H_s^2 T_e \quad (11)$$

By taking sea water mass density as 1025 kg/m<sup>3</sup> and gravitational acceleration as 9.81 m/s<sup>2</sup>, the above equation can be further simplified as shown in Equation (12). When

the significant wave height is given in meters and energy period in seconds, the calculated wave power is in kilowatts per meter of the wave front length (kW/m).

$$P \approx 0.49H_s^2T_e \quad (12)$$

It should be noticed, that there is a significant uncertainty of wave power estimation particularly when the sea state consists of multiple wave systems (Example: when the swell waves are approaching with a different direction compared to local sea waves). However, the effect of errors in wave period will be significantly smaller than the effect of errors in wave heights since wave power  $P \propto H_s^2T_e$ .

## **2.5 Regional-scale wave energy assessments**

### **2.5.1 Mediterranean Sea**

Liberti et al. (2013) assessed spatial variation of wave energy resource in the Mediterranean Sea using numerically simulated wave data. Their study prompted to identify the areas where wave energy resource is most promising in the Mediterranean Sea. The Sicily Channel and the western Sardinia coasts are found to be the most appropriate coastal regions for wave energy harvesting based on the wave power distribution. They have extended the investigations for a set of selected sites to examine the behavior of wave heights, wave periods and wave directions.

### **2.5.2 Southern Caspian Sea**

The Caspian Sea is known as the largest enclosed water body which is located between Europe and Asia. It has about 78 200 km<sup>3</sup> water volume bordering by Russia, Azerbaijan, Iran, Turkmenistan and Kazakhstan. Kamranzad et al. (2016) evaluated wave energy resource in the Southern Caspian Sea. They investigated temporal as well as spatial variation of energy resource in that region, thus allowing them to identify wave energy hotspots and the stability of the source over time.

Wave projections for 11 years which were obtained using SWAN wave model, were used in this study. They have selected four nearshore sites to assess the feasibility of wave energy harvesting based on monthly and seasonal variations of wave power. Monthly and seasonal variability indices were used to quantitatively evaluate the stability of the resource. Finally, they have concluded that the central station is the most feasible location for wave energy harvesting in the Caspian Sea.

### **2.5.3 Peninsular Malaysia**

Mirzaei et al. (2016) assessed wave energy potential along the east coast of Malaysia using simulated waves over a period of 31 years since 1979. They investigated the seasonal and inter-annual variation of the resource and established a correlation between wave power fluctuation with local climate variabilities. Also, they highlighted the inter-annual wave power fluctuations due to the El Niño-Southern Oscillation (ENSO). It was found that the northern part of the coast is more energetic than the southern coast (Figure 2.10). The sheltering effect of the islands was found to be the reason for this variation.

### **2.5.4 Canary Islands**

Gonçalves et al. (Gonçalves M., Martinho P., Soares C.G., 2014) assessed wave energy potential around Canary Islands using numerically projected ocean waves from SWAN spectral model and WAVEWATCH III model. The modeled outputs were validated using satellite data for one year and buoy data for a three-year period.

The average wave power was found as around 25 kW/m which can be considered as a little bit lower value comparing with the other energetic locations in the Atlantic European coast (Figure 2.11). Further, they have characterized the wave power at different selected sites and concluded that the wave energy is concentrated between 1.5m and 3.5m in significant wave height and 7 s and 13 s in energy period.



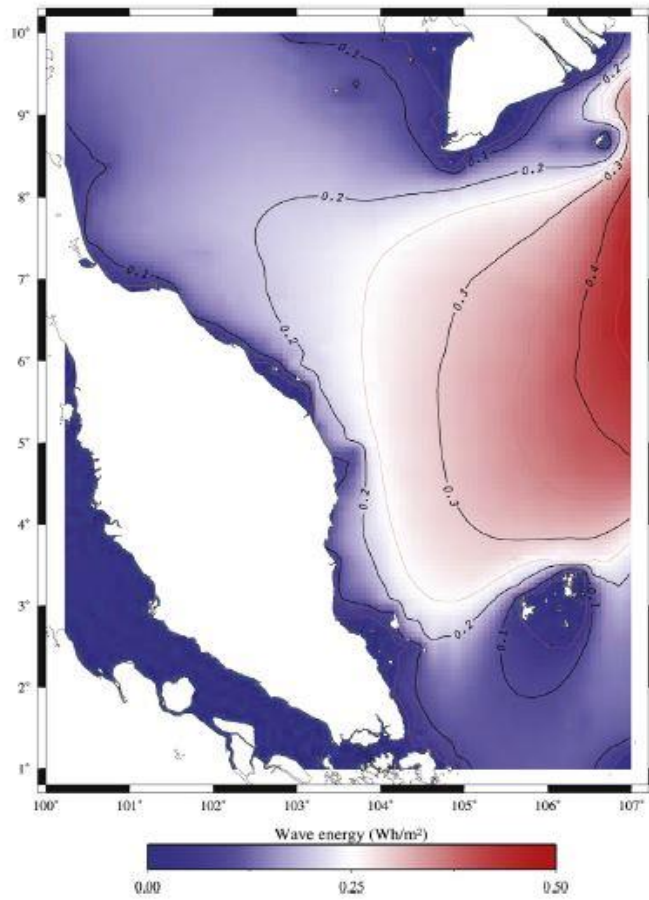


Figure 2.10: The annual mean spatial distribution of wave energy around Malaysia (Source: (Mirzaei A., Tangang F, Juneng L., 2016)

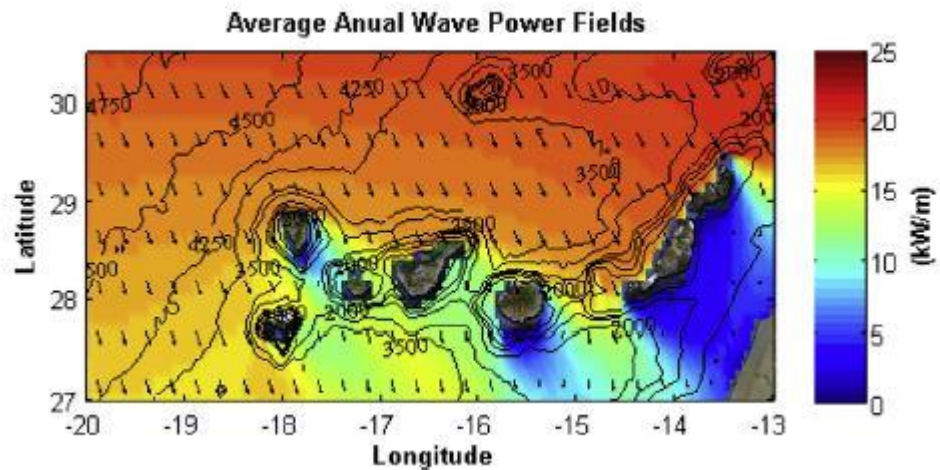


Figure 2.11: Average annual wave power along the Canary Islands (Source: (Gonçalves M., Martinho P., Soares C.G., 2014))

### 2.5.5 Shandong peninsula, China

Liang et al. (2013). carried out a spatio-temporal wave energy resource evaluation in a small coastal area in China using simulated wave data for 16 years, focusing mostly on areas close to the shoreline. The wind data input for the wave model derived by the Weather Research and Forecasting Model (WRF) was used for the wave model. They have conducted their analysis under both mean and extreme wave conditions. Further analysis has been carried out for selected three sites characterizing wave state parameters. Also, wave power roses were introduced to examine the dominant wave direction for selected sites.

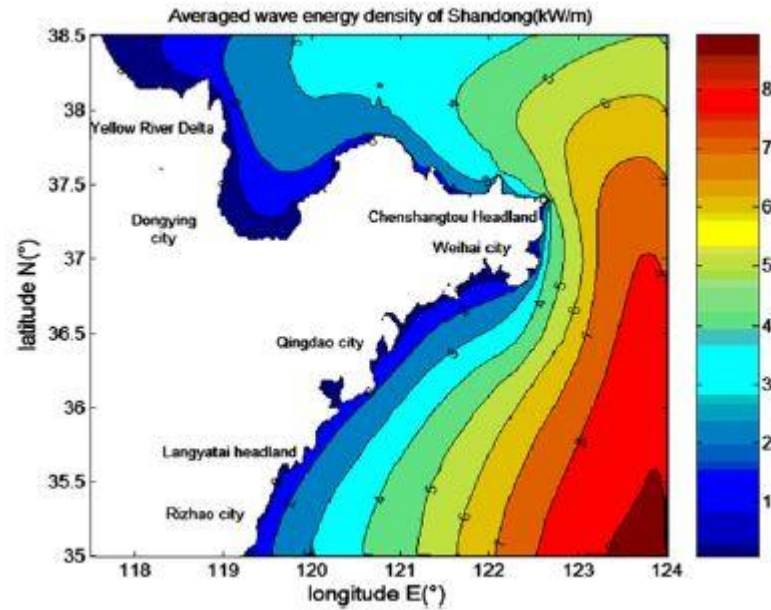


Figure 2.12: Distribution of average wave energy density (kW/m) in Shandong-China  
(Source: (Liang B., Fan F., Yin Z., Shi H., Lee D., 2013)

### 2.5.6 Other similar studies on wave energy potential

Similar studies have been done in numerous other countries around the world, who are interested in investigating wave energy harvesting potential. Some of the referred studies are listed below.

- Folley and Whittaker for UK (Folley M., Whittaker T.J.T., 2009)
- Iglesias et al. for Spain (Iglesias G., Lopez M., Carballo R., Castro A., and Fraguera J.A. , 2009)
- Iglesias and Carballo, 2010 – France (Iglesias G. and Carballo R., 2010)
- Hughes and Heap, 2010 – Australia (Hughes M.G. and Heap A.D. , 2010)

## **2.6 Wave energy assessments for Sri Lankan region**

Studies on wave energy resource in the Indian Ocean is rare except for regional studies focusing mainly on coastal areas of India (Aboobacker (Aboobacker V.M., 2017); (Sanil K. V., Anoop T. R., , 2015) and Iran (Kamranzad et al., (Kamranzad B., Shahidi A. E., Chegini V., Bakhtiary A. Y., 2015).

In a recent study, Kamranzad and Mori (Kamranzad B, Mori N., 2019) introduced a new identifier to specify areas with higher energy stability considering both short-term fluctuations such as monthly variation and long-term changes due to the climate change and applied it to the nearshore areas of the Indian Ocean. The distribution of the suggested identifier indicated that the south-western to south-eastern coastal areas of Sri Lanka have a high energy potential and stability in both short and long-term (Gunaratne P.P., Ranasinghe D.P.L., Sugandika T.A.N. , 2011).

Sri Lanka, being an island located in the Indian Ocean is exposed to energetic wave conditions all year round thus making wave energy a potential renewable energy resource to supplement the country's ever-growing demand for green energy. Chamara and Vithana (Chamara R.N., Vithana H.P.V, 2018) analysed nearshore wave energy resource along the south-west and south coasts of Sri Lanka using a numerical model forced by offshore Galle wave measurements of Sheffer et al., (Sheffer H.J., Fernando K.R.M.D., Fittschen T., 1994). However, their analysis was limited to a very short period of time and to one sea bed contour and therefore unable to be used to determine spatial and temporal variability and stability of the resource.

Amarasekera et al. (Amarasekera H.W.K.M., Abeynayake P.A.G.S., Fernando, M.A.R.M., Aputharajah A., Uyanwaththa, D.M.A.R., Gunawardena S.D.G.S.P, 2014) carried out a feasibility study of ocean wave power in the south coast of Sri Lanka using numerically generated waves from WAVEWATCHIII model. They concluded that installation of small-scale wave energy devices can be feasible. However, it is not clear if swell waves were taken into account in their analysis.

## **2.7 Impact of global climate change on wave energy resource**

Most reported studies have been focused on assessing the currently available wave resource and its fluctuation over timescales from seasonal to a few decades. However, wave resource can be significantly influenced by global climate change which can be felt at timescales over a few decades to centuries (Harrison G.P. and Wallace A.R., 2005). The design life of a wave energy development will, in general, surpasses a few decades, it is important to investigate potential long-term variations of available wave energy resource that linked with global climate change.

Although short- to medium-term variabilities of future wave energy resource may be evaluated by extrapolating historic trends of variations determined by observed wind and wave data or by wind or wave hindcasts, long term impacts of global climate change can only be assessed using future wave projections that are determined using atmospheric outputs from Global Climate Models (GCMs) or high-resolution Regional Climate Models (RCMs). Mackey et al (Mackay, Edward B.L., Bahaj, AbuBakr S., Challenor, and Peter G., 2010) examined climate change impacts on ocean wave climate on the predictability of wave power in an area off the north coast of Scotland using hindcast wave data for the fifty-year period between 1954 and 2004. They concluded that anthropogenic climate change impacts over a lifetime of a wave farm may be smaller than the natural variability.

However, it should be noted that their conclusion has been made based on hindcasts of historic waves at a time where global climate variabilities may be smaller than the most recent predictions. As a result, the validity of their conclusion may not hold true in future where global climate and its impacts on the oceans rapidly varies in time (IPCC 2018). Reeve et al. (Reeve D.E., Chen S., Pan S., Magar V., Simmonds D.J. and Zacharioudaki A., 2011), using wave forecasts based on IPCC A1B and B1 wind scenarios between 2061 and 2100, found that available wave power in the south-west of the UK will decrease by 2-3% in future. Charles et al. (Charles E., Idie R.D., Deleclus P., Deque. M., Le Cozannet G., 2012), using numerically simulated future waves, reported that wave height in the Bay of Biscay, France will be decreased in future as a result of global climate change.

Kamranzad et al. (Kamranzad B., Shahidi A. E., Chegini V., Bakhtiary A. Y., 2015) investigated the climate change impacts on wave energy resource in the Persian Gulf, using future wave projections derived based on atmospheric wind outputs from a global climate model, covering a 30-year period from 2071 to 2100. They found that wave energy resource in the Persian Gulf will notably change in the future and the amount of variability depends on the global climate change scenario.

Woolf and Wolf (Wolf. J., and Woolf. D., 2006) concluded that there is no clear pattern of how the global wave climate will respond to future climate variabilities. Wolf and Woolf (2006) stated, based on climate model predictions of the North Atlantic Oscillation, that wave heights in the North Atlantic are likely to be larger in future. However, they noted the need for further studies to confirm this observation.

Based on wave projections from a super-high-resolution model, Kamranzad and Mori (Kamranzad B, Mori N., 2019) concluded that the Northern Indian Ocean will have less stable wave climate while the opposite is true for the Southern Indian Ocean. They also found that while wave periods will not notably change in future, significant wave heights will be affected by the future change in the Indian Ocean monsoons. Bashkaran et al. (Bhaskaran, P.K., Gupta, N. and Dash, Mihir., 2014), using wind-generated wave climate derived based on satellite observations, postulated that waves in the Northern Indian Ocean will be increased in future as a result of increasing wave activity in the Southern Indian Ocean due to global climate change.

As described above, many studies have conducted in order to find the impacts of climate change towards the wave energy resource.

### 3.0 RESEARCH METHODOLOGY

#### 3.1 Introduction

This section describes the methodology followed in the study. Initially, a literature review was conducted and then based on that an appropriate wave model was selected. Then the ocean waves were modeled and modeled data were analysed. Based on the modeled wave data, spatial and temporal variations of wave energy resource were evaluated in different time scales. As the next step, the stability and sustainability of wave energy resource were assessed in changing climate conditions using future wave projections. Finally, the conclusions were made based on the results.

#### 3.2 Methodology flow chart

The methodology is described in Figure 3.1

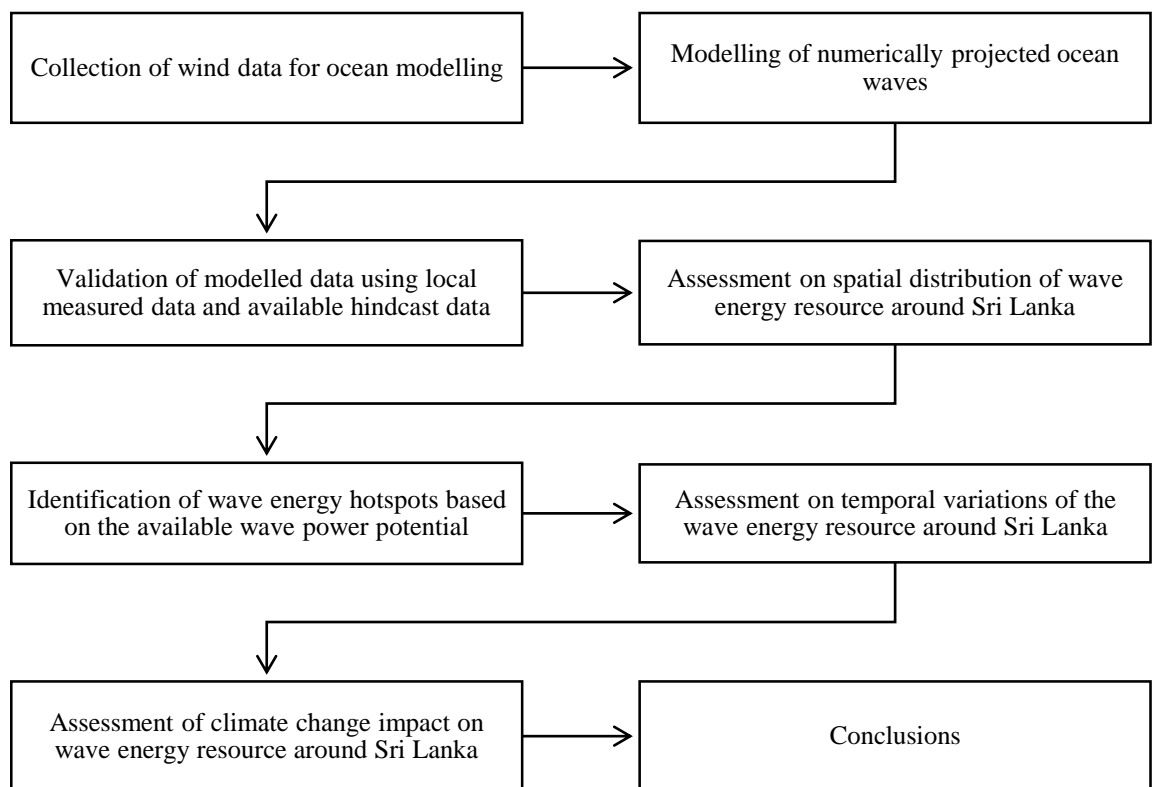


Figure 3.1: Research methodology flow chart

## **4.0 WAVE MODEL AND MODEL VALIDATION**

### **4.1 Introduction**

This chapter includes the preparation of the wave model and its validation process. The first part of the chapter briefly describes the process of the development of the wave model. Then a detailed description of the available local measured data sets is given. Then the modeled outputs were obtained and validated with the measured data sets and hindcast data to check the accuracy and reliability of the model. Finally, the last part of the chapter describes the applicability of the selected model towards the wave energy assessment in the Sri Lankan region.

### **4.2 Process of the development of the wave model**

The wave projections were obtained through a numerical wave model developed using Simulating Waves Nearshore (SWAN) software. It was driven by the atmospheric forcing generated by a Global Climate Model (GCM). The model was run in time slices in the time domain representing the "present" and "future"(at the end of the century) wave climates to evaluate and compare the current and future wave power of Sri Lanka.

A cascade of computational wave models was used to obtain the wave projections around Sri Lanka. The waves have been simulated using wind outputs from the super high-resolution Atmospheric Global Climate Model (AGCM) of the Japan Meteorological Agency, MRI-AGCM3.2S (Mizuta R., Yoshimura H., and Murakami H., 2012). The future climate scenario based on Representative Concentration Pathway (RCP 8.5), as defined by representing trajectories of increasing global radiative forcing reaching  $+ 8.5 \text{ W m}^{-2}$ , by the year 2100 compared to pre-industrial conditions, was used (Hibbard K.A., Meehl G.A., Cox P.M., Friedlingstein P., 2007). These outputs were first used to develop an Indian Ocean wave model (KU\_IO), as reported in detail in Kamranzad and Mori (Kamranzad B, Mori N., 2019), using SWAN spectral wave model (Booij N., Ris R.C., Holthuijsen L.H., , 1999). The KU\_IO model domain covers the area between 20°E-90°E in longitude and 71°S-30°N



in the latitude of the Indian Ocean. The spatial and temporal resolution of wind inputs were 20 km and 1 hr, respectively.

The wind source term required for generating waves in the wave model was calculated following Komen et al. (Komen, G.J., Hasselmann, S., Hasselmann, K., 1984). Non-linear quadruplet wave-wave interaction formulation of Hasselmann et al (Hasselmann, H. and Hasselmann, K., 1985). was used. The frequency domain consists with 36 bins of frequencies from 0.03 to 1 Hz on a logarithmic scale. The directional computational grid was divided into 36 bins of  $10^\circ$ . The KU\_IO wave model has been extensively validated using numerous satellite-derived historic wave data in the whole computational grid of the Indian Ocean. The validation results reveal that the model is capable of simulating the current wave climate of the entire Indian Ocean very satisfactorily. An extensive description of the model development, calibration and validation are given in Kamranzad and Mori (Kamranzad B, Mori N., 2019). The KU\_IO model was used to generate significant wave height ( $H_s$ ), mean spectral wave period  $T_{m01}$  and wave direction for two 25-year time slices; (i) between 1979-2003, representing the ‘present’ wave climate and, (ii) between 2075-2099, representing the ‘future’ wave climate.

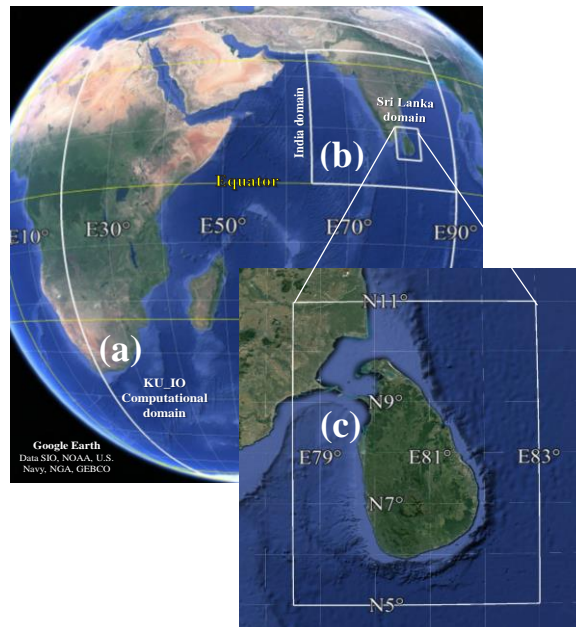


Figure 4.1: (a) Indian Ocean KU\_IO, (b) KU\_IND and (c) KU\_SLK wave model domains used to generate wave projections for the Sri Lanka region

KU\_IO wave model predictions provided boundary conditions for a smaller, India regional scale wave model (KU\_IND) that covers 64°E-90°E and 0-26°N region with spatial resolution of 0.166° x 0.166°, which generated 25 years ‘present’ and ‘future’ wave climate at 6 hr intervals. Finally, a small-scale Sri Lanka local model (KU\_SLK) (5°-11°N, 79.5°-83.5°E) was nested to the India regional wave model to determine high-resolution ocean wave climate around Sri Lanka for the same ‘present’ and ‘future’ time-periods. The spatial resolution of the Sri Lanka model domain was 0.05° x 0.05° (5.56 km x 5.56 km) and the outputs were generated with the same temporal resolution as that of the India regional model. The three model domains used for wave simulations are shown in Figure 4.1. The models use GEBCO seabed bathymetry data with 30 arc-second spatial resolution ([https://www.gebco.net/data\\_and\\_products/gridded\\_bathymetry\\_data/](https://www.gebco.net/data_and_products/gridded_bathymetry_data/)) (Weatherall P., Marks K. M. , Jakobsson M., Schmitt T., Tani S, Arndt J. E., 2015).

### **4.3 Model validation**

Although the KU\_IO model, which provided boundary conditions for the Sri Lanka regional model has been extensively validated, the Sri Lanka regional model was validated against two data sources before being used for projecting long term wave data. The first source is the measured waves at Galle between 1989 and 1992. The second source is ERA-Interim Global Atmospheric Reanalysis wave data produced by the European Centre for Medium-range Weather Forecasts (ECMWF) (<https://apps.ecmwf.int/datasets/>).

Modelled and ERA-Interim Reanalysis wave data at the closest available Galle wave measurements location and two more locations around the west and south coasts of Sri Lanka were selected for comparisons. All locations corresponding to the data used in the model validation are summarised in Figure 4.2 and Table 4.1. Although wave measurements at Matara are available in 2013/2014, forcing required to run the wave model for this period is not available. Therefore, it wasn’t possible to use Matara data for wave model validation.

Table 4.1: Details of all data locations used for wave model validation

Details of the data set		Approximate Water Depth	Location	Duration	Frequency
Galle	Measured	70 m	5.93 N, 80.23 E	1/2/1989 – 19/9/1992	3hr
	Modelled	70 m	5.9313N, 80.2324E	1/2/1989 – 19/9/1992	1hr
	ERA-Interim	40 m	6.000N, 80.250E	1/2/1989 – 19/9/1992	6hr
P1	Modelled	75 – 100 m	6.750N, 79.750E	1/1/1999 – 31/12/2003	6hr
	ERA-Interim	75 – 100 m	6.750N, 79.750E	1/1/1999 – 31/12/2003	6hr
P2	Modelled	75 – 100 m	6.250N, 81.750E	1/1/1999 – 31/12/2003	6hr
	ERA-Interim	75 – 100 m	6.250N, 81.750E	1/1/1999 – 31/12/2003	6hr

Figure 4.3 gives a direct comparison of measured (at GE in Figure 4.2) and modelled (at GMO in Figure 4.2) significant wave height time series for the period of 4 years between 1989 and 1992. It can be seen that the model is able to capture the significant wave heights and their temporal variations at this location accurately although some extreme wave events have been missed. This may be attributed to the model not being able to capture some locally generated high energy events, potentially as a result of the selected resolution of the wave model and the wind forcing used.

A comparison of monthly averaged modelled, measured and ERA-Interim Reanalysis significant wave heights determined for the same period is shown in Figure 4.4. The results reveal that the measured and modelled monthly averaged significant wave height values are well in agreement [Root Mean Square Error (RMSE) = 0.12m]. The model slightly over-predicted monthly averaged significant wave heights only in January and February. ERA-Interim Reanalysis monthly averaged wave heights are

smaller than the measured and modelled values between July and September but in agreement in all other months.

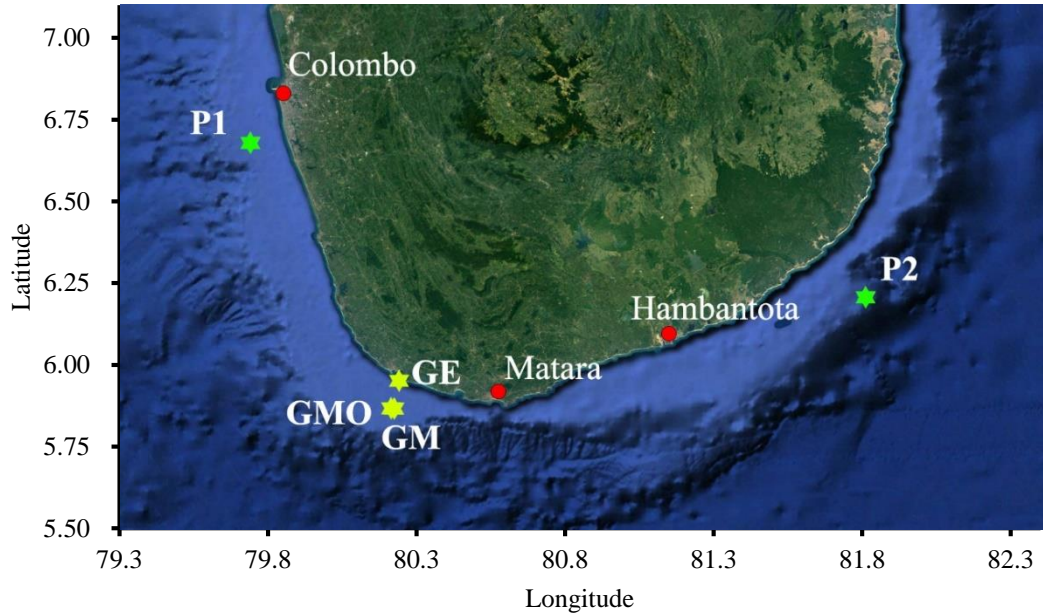


Figure 4.2: Map with all data locations used for wave model validation. GMO – Galle (Modelled), GE - Galle (ERA-Interim), GM - Galle (Measured) P1 and P2 are additional model validation points

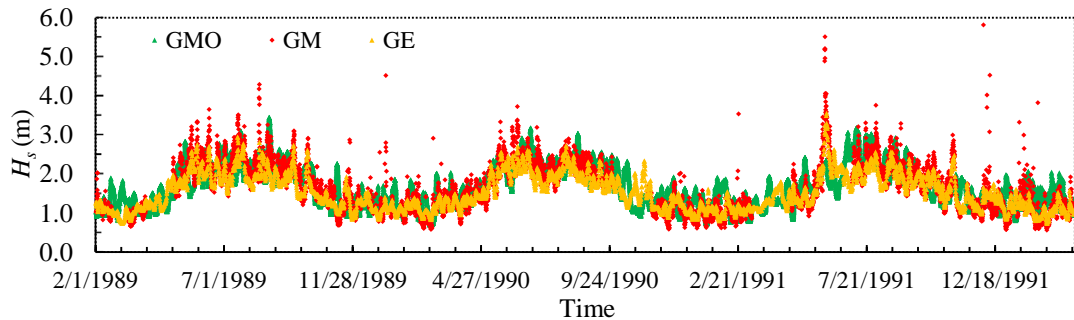


Figure 4.3: Comparison of modelled [at GMO, (5.93° N 80.23° E)] (green), ERA-Interim Reanalysis [at GE (6.0N, 80.250E)] (yellow) and measured [at GM (5.93 N, 80.23E)] (red) wave height time series

The modelled monthly averaged  $T_{m02}$  values for months June-August seems to be significantly lower (maximum of 35%) than the measured data although they are comparable during the rest of the year (Figure 4.5). It should be noted that SWAN

wave model structurally underestimates mean and peak wave periods by 10%-20% (Team, 2017). The sensitivity of  $T_{m02}$  to very high-frequency waves should also be noted. The model may not capture very high-frequency wind sea that dominates the local wave climate during the monsoon season. However, it is worth mentioning that waves with very high frequencies are not important for wave energy resource studies as most extractable energy is concentrated at lower frequencies. Monthly averaged ERA-Interim Reanalysis

wave periods are significantly higher than both measured and modelled wave periods except in the months of June and July.

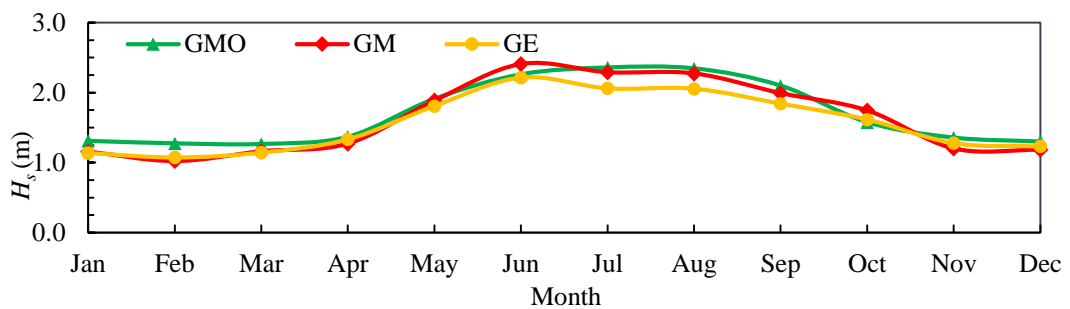


Figure 4.4: Comparison of modelled [at GMO, (5.93° N 80.23° E)] (green), ERA-Interim Reanalysis [at GE (6.0N, 80.250E)] (yellow) and measured [at GM (5.93 N, 80.23E)] (red) monthly average significant wave heights

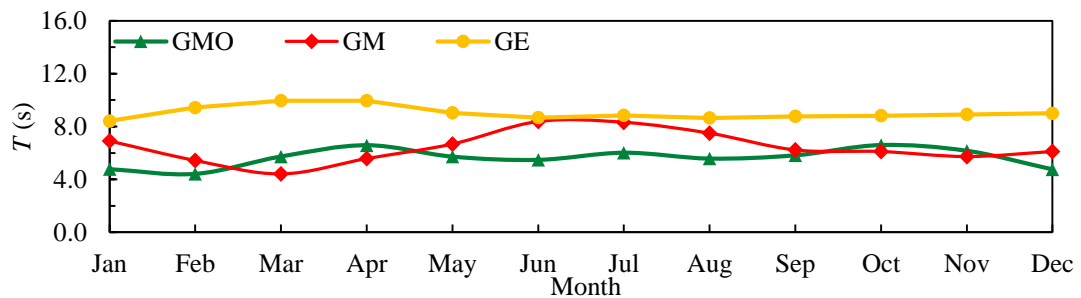


Figure 4.5: Comparison of modelled [at GMO, (5.93° N 80.23° E)] (green), ERA-Interim Reanalysis [at GE (6.0N, 80.250E)] (yellow) and measured [at GM (5.93 N, 80.23E)] (red) monthly average wave period

To supplement wave model validation against measured data at Galle, modelled waves at two other locations (P1, P2 – Figure 4.2) in the west and south coasts of Sri Lanka are compared with ERA-Interim Reanalysis wave data. In Figure 4.6, a direct comparison of modelled and ERA-Interim Reanalysis significant wave heights at

points P1 and P2 is given (Black dark line gives  $x = y$  line while black dotted lines give 80% confidence interval. The red dotted line gives the linear fit). The maximum deviation between the two data sets is 1.5m at both locations, except for a small number of outliers found at P1. The gradient of the linear trend lines at P1 and P2 are 0.94 and 1.1 respectively. RMSE between the two datasets at P1 and P2 are 0.4 m and 0.5 m respectively.

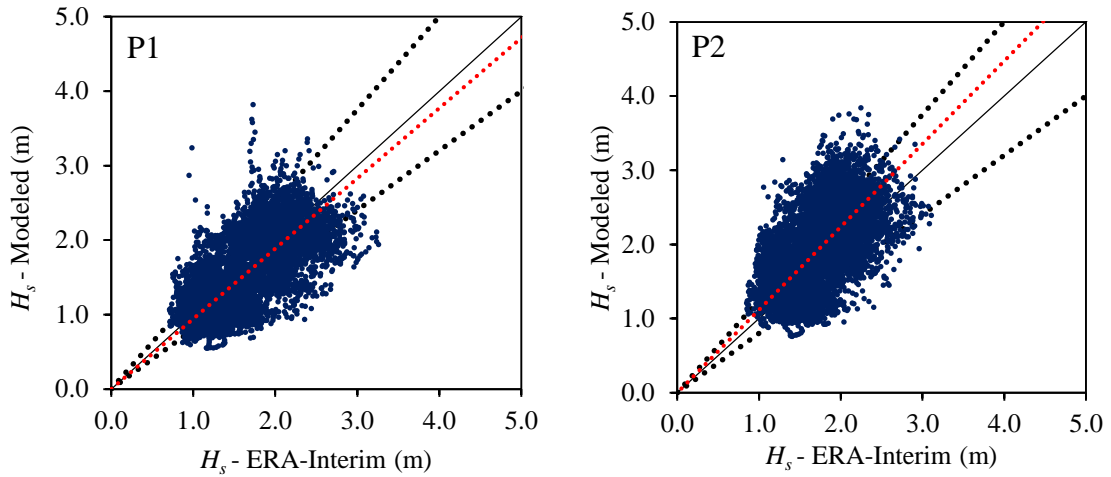


Figure 4.6: A comparison of ERA-Interim data and modelled significant wave heights during the period 1999-2003 at points P1 and P2

A figure similar to Figure 4.6 for the wave period is shown in Figure 4.7.  $T_{m-10}$  of modelled data and mean wave period of ERA-Interim data are used for comparison as that  $T_{m-10}$  is the most appropriate representative wave period for wave power calculations. This figure reveals that although the maximum deviation between modelled and ERA-Interim Reanalysis  $T_{m-10}$  values are large the gradient of the trendlines at P1 and P2 are 0.92 and 0.91 respectively while RMSE between the two datasets at P1 and P2 are 1.6 s and 1.7 s respectively.

Figure 4.8 shows monthly averaged (averaged over the period between 1999 and 2003 used for comparisons) significant wave height and mean energy period for P1 and P2. Modelled an ERA-Interim reanalysis monthly averaged significant wave heights at P1 are in very close agreement (RMSE = 0.09m), although they are in slightly less agreement at P2 (RMSE = 0.23m). However, the comparison of modelled monthly averaged significant wave heights with that of measured values at Galle revealed

(Figure 4.4 above) the model captured measured waves accurately, which reassures the performance of the model in capturing significant wave heights correctly. Modelled an ERA-Interim reanalysis monthly averaged mean energy periods at both P1 and P2 are in good agreement. RMSE at P1 is 0.7 s while that at P2 is 0.8 s.

The good agreement between the two wave models reassures the fact that the model

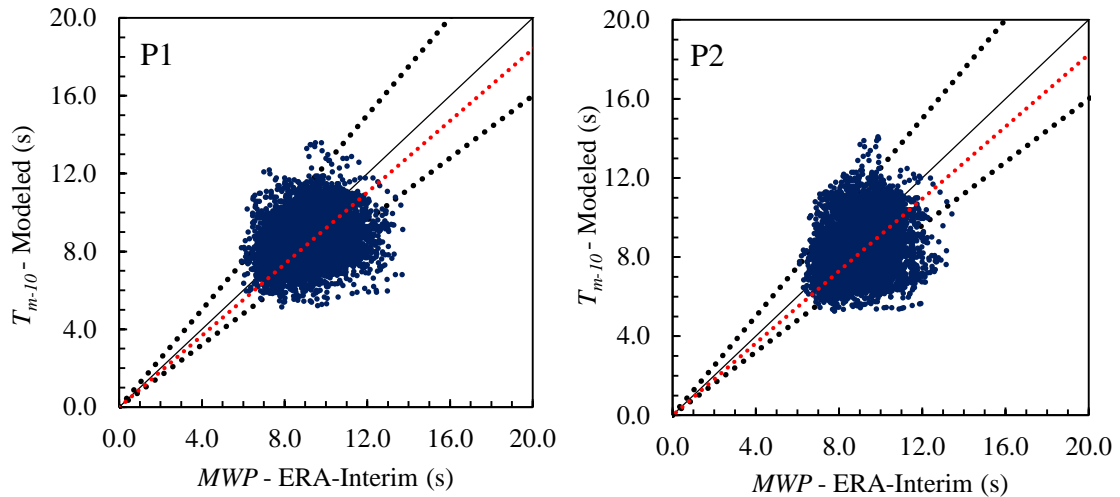


Figure 4.7: A comparison of modelled and ERA-Interim Reanalysis mean energy period during the period 1999-2003 at points P1 and P2

used in this study is capable of capturing the wave climate in the west and south of Sri Lanka. Considering that the Northern Indian Ocean being one of the most climatologically complex and dynamic areas in the world as a result of the seasonally reversing tropical monsoon system operating in this region (Anoop, T.R., Kumar, V.S., Shanass, P.R. and Johnson, G., 2015), the above comparisons revealed that the wave model satisfactorily captured the Sri Lanka wave climate around Sri Lanka. The validated wave model is then used to generate wave projections for two 25-year period time slices as at 6hr intervals.

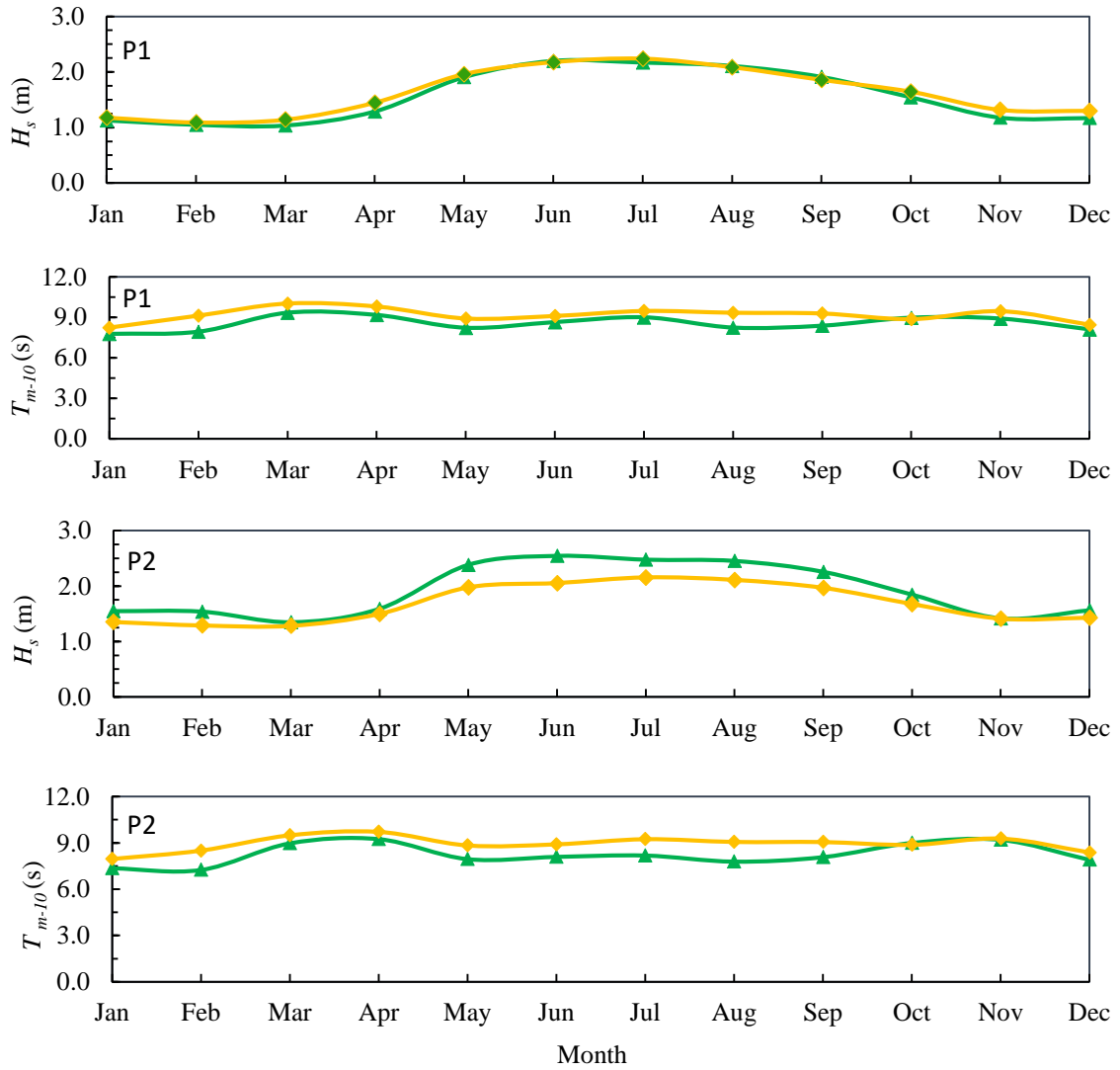


Figure 4.8: A comparison of modelled (green) and ERA-Interim Reanalysis (yellow) monthly averaged significant wave height and mean energy period during the period 1999 and 2003 at points P1 (top) and P2 (bottom)



## 5.0 EVALUATION OF SPATIO-TEMPORAL VARIABILITY OF WAVE ENERGY RESOURCE

### 5.1 Introduction

Twenty-five-year wave projections from 1979 to 2003 that represent the current prevailing wave climate in the Sri Lanka region is used in this analysis and wave data from all grid points of the Sri Lanka regional wave model grid points are used. Wave power was determined from Equation (13), using the mean energy period ( $T_{m-10}$ ) given in Equation (14) to accommodate the randomness of the wave climate (MARINET, 2015).

$$P = 0.49H_s^2T_{m-10} \quad (13)$$

in which  $H_s (= H_{m0} = 4\sqrt{m_0})$  is the significant wave height determined from the wave spectrum.  $T_{m-10}$  is the energy period given by Equation (14)

$$T_{m-10} = \frac{m_{-1}}{m_0} \quad (14)$$

in which  $m_{-1}$  is the first negative spectral moment of the wave frequency spectrum.

### 5.2 Wave power distribution around Sri Lanka

#### 5.2.1 Spatial distribution of wave power

Figure 5.1 reveals that a substantial amount of wave power is available around the coast from west to south-east of Sri Lanka. The average wave power available in this region is comparable to some of the very high wave energy resource locations found around the world (Hughes M.G. and Heap A.D., 2010) (Neill N.P., Vogler A., Goward-Brown A.J., Baston S., Gillibrand P.A., Walkdon S., Woolf, D.K., 2017). It can also be seen that available wave resource broadly varies from the offshore to

nearshore. The north-west to the east coastline contains considerably less amount of wave power, mainly as a result of limited fetch and sheltering by mainland India.

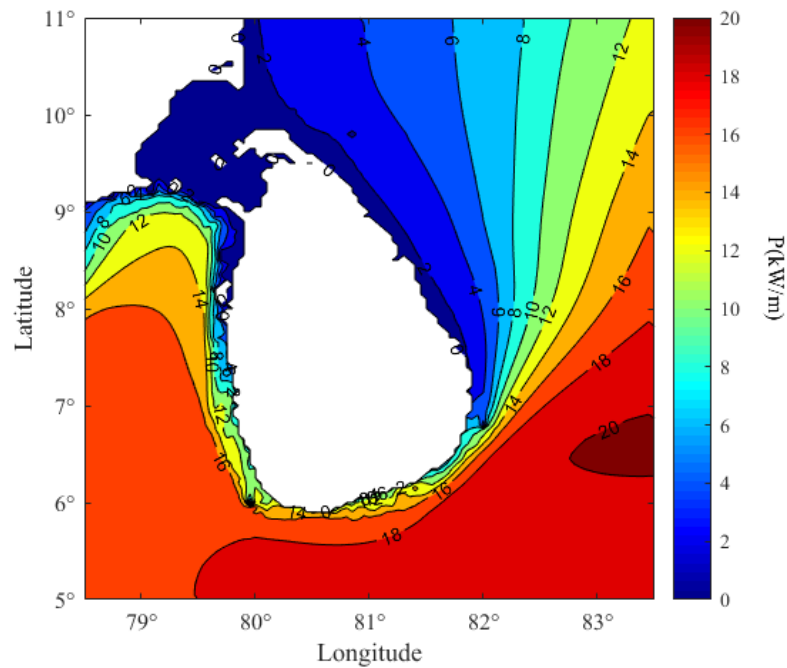


Figure 5.1: A spatial distribution of average wave power (averaged over the simulated 25-year period between 1979 and 2003) for the Sri Lankan domain

Although a high level of wave power is available in the southern part of Sri Lanka, a strong monthly to seasonal variation is expected as a result of monsoons operating in the Sri Lanka region. To investigate the variation of available wave power with the time, which is important to examine the reliability of the energy source, spatial variation of monthly averaged wave power was investigated (Figure 5.2). Wave projections of all twenty-five years were used for the averaging.

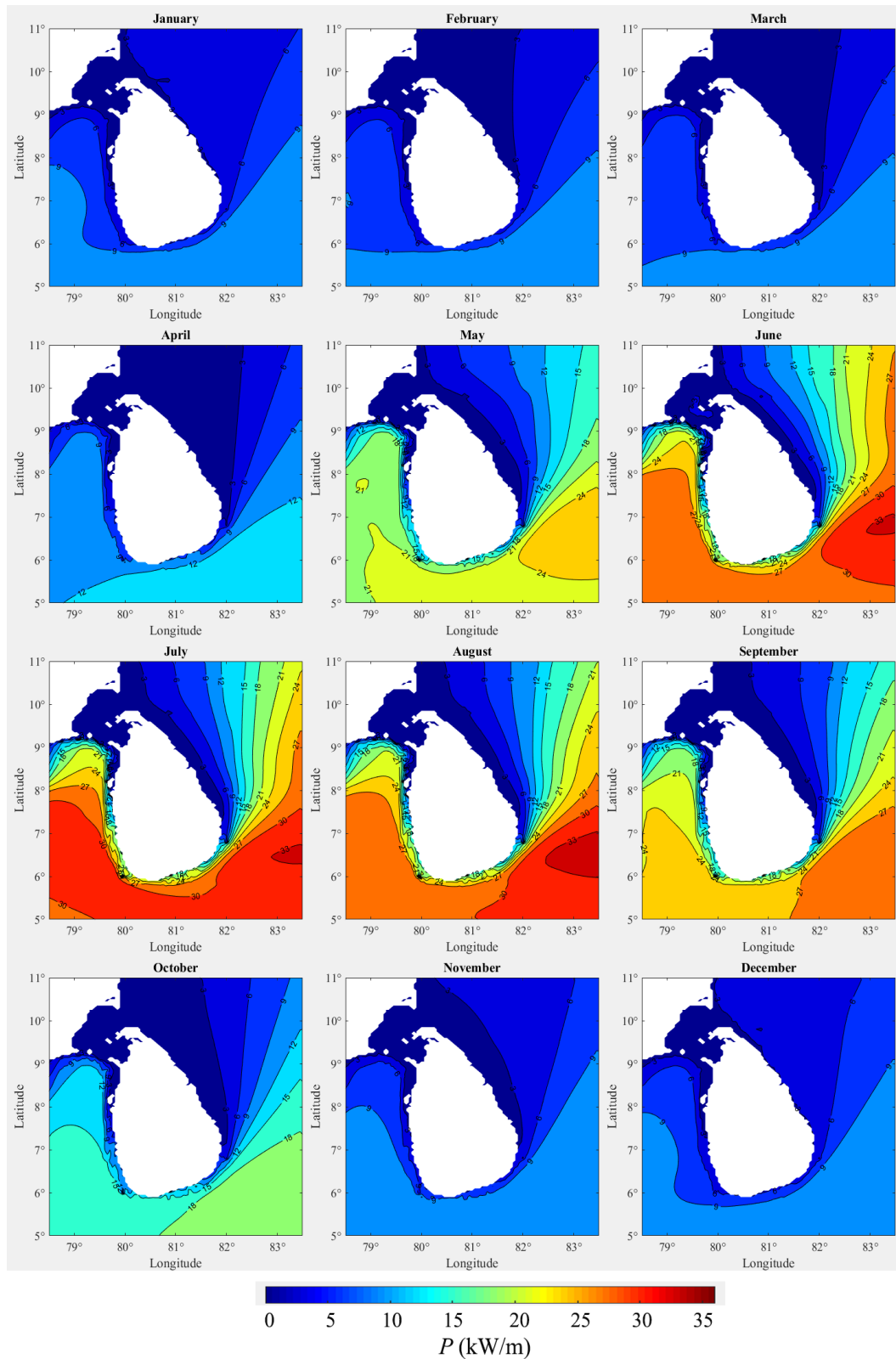


Figure 5.2: Spatial distribution of monthly average wave power (averaged over the modelled 25-year period between 1979-2003) for the entire coastline of Sri Lanka

In line with the south-west monsoon, the available monthly averaged wave power from May to September is significantly higher in the southern region of Sri Lanka (25-30 kW/m) than that during the rest of the year (5-15 kW/m), as a result of the superposition of incoming swell with locally generated wind sea. However, the available monthly averaged wave power in the south-west to south-east region exceeds 10 kW/m all year round. The available wave power in all other areas is less than 5 kW/m. Therefore, the south-west to south-east coastal regions of Sri Lanka will be specially focused in this study.

### 5.2.2 Temporal and directional variations at selected sites

Although the available wave power and its seasonal variation seem to be broadly uniform along the south-west to the south-east coast of Sri Lanka, spatial variation of the width and depths of the narrow continental shelf, direction of wave approach relative to the coast and wave transformation processes taking place as a result of local variabilities of the seabed may induce localized spatial variabilities to the available wave power. Therefore, eighteen locations around the coast from south-west to south-east coast, covering nine offshore and nine nearshore locations, were selected for a

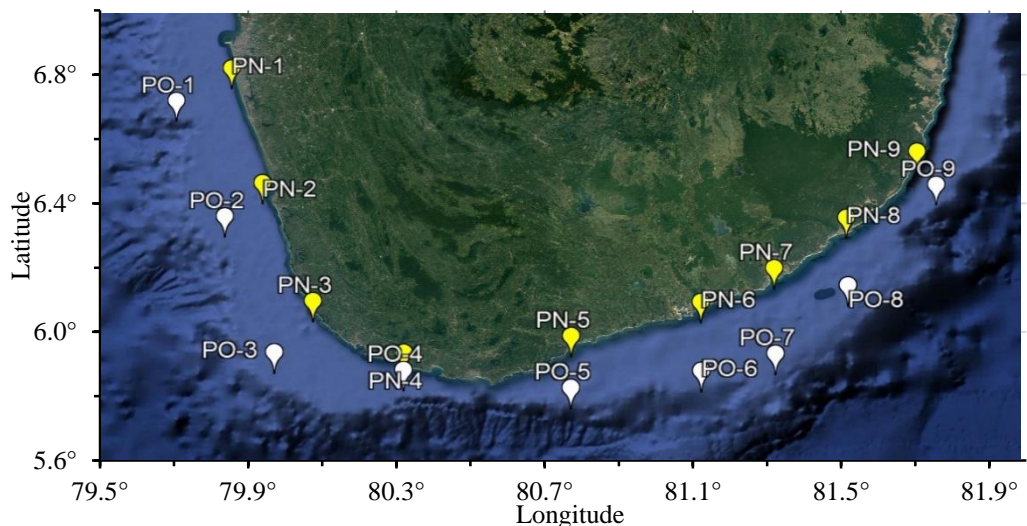


Figure 5.3: Eighteen nearshore (PN-1 to PN-9) and offshore (PO-1 to PO-9) locations selected along the south-west to south-east coast of Sri Lanka for detailed wave resource analysis.

detailed analysis of spatio-temporal variability of wave power in this region (Figure 5.3).

All selected nearshore points are located between the 20m and 30m water depths and at a distance less than 2.5km from the shoreline while offshore points are located between 60m and 100m water depth and at distances between 7-25km from the shoreline. All offshore points are located on the continental shelf.

The available wave power at the selected nearshore and offshore locations are shown in Figure 5.4 and Figure 5.5, respectively. According to these figures, there is a considerable spatial variation of wave power along the coast from south-west to south-east. The highest level of available offshore wave power is available in the south-west and south (PO-3 to PO-7). A significant proportion of wave power at these points falls within the 20-30 kW/m band. On the other hand, at points PO-8 and PO-9, most power falls between the 10-20 kW/m. The dominant direction is mostly south and south-west, however, a small amount of power is available from the waves reaching from the south-east at PO-8 and PO-9. Meanwhile, as can be seen in Figure 5.4, the predominant direction at all nearshore points is south-west, PN-3 and PN-9 being the only exceptions where the predominant direction is the south. Also, the transfer of power into different bands can be observed as a result of nearshore wave transformation processes

The seasonal stability of locally available wave power is an important aspect in making decisions related to wave energy developments and device selection. Box-Whisker plots given in Figure 5.6 and Figure 5.7 give monthly variability of wave power as well as the range of variability within a month (The plot was produced using the 25 years (1979-2003) projected wave data). Top, middle and bottom black lines of the boxes give the third quartile, median and first quartile of wave power determined from all twenty-five years of wave projections between 1979 and 2003. The results reveal that during the south-west monsoon period, where larger wave power is available, the range of variability of wave power is also higher than the rest of the year at all locations. This is attributed to the highly variable sea waves generated by the south-west monsoon. The range of variability of available offshore wave power differs along the coastline where the highest variability is found in the south-west and south of Sri

Lanka (PO-1 to PO-7). Nearshore locations seem to follow a similar trend although the range of variability is significantly smaller, understandably due to local transformation and dissipation processes that may occur in the nearshore as mentioned above.

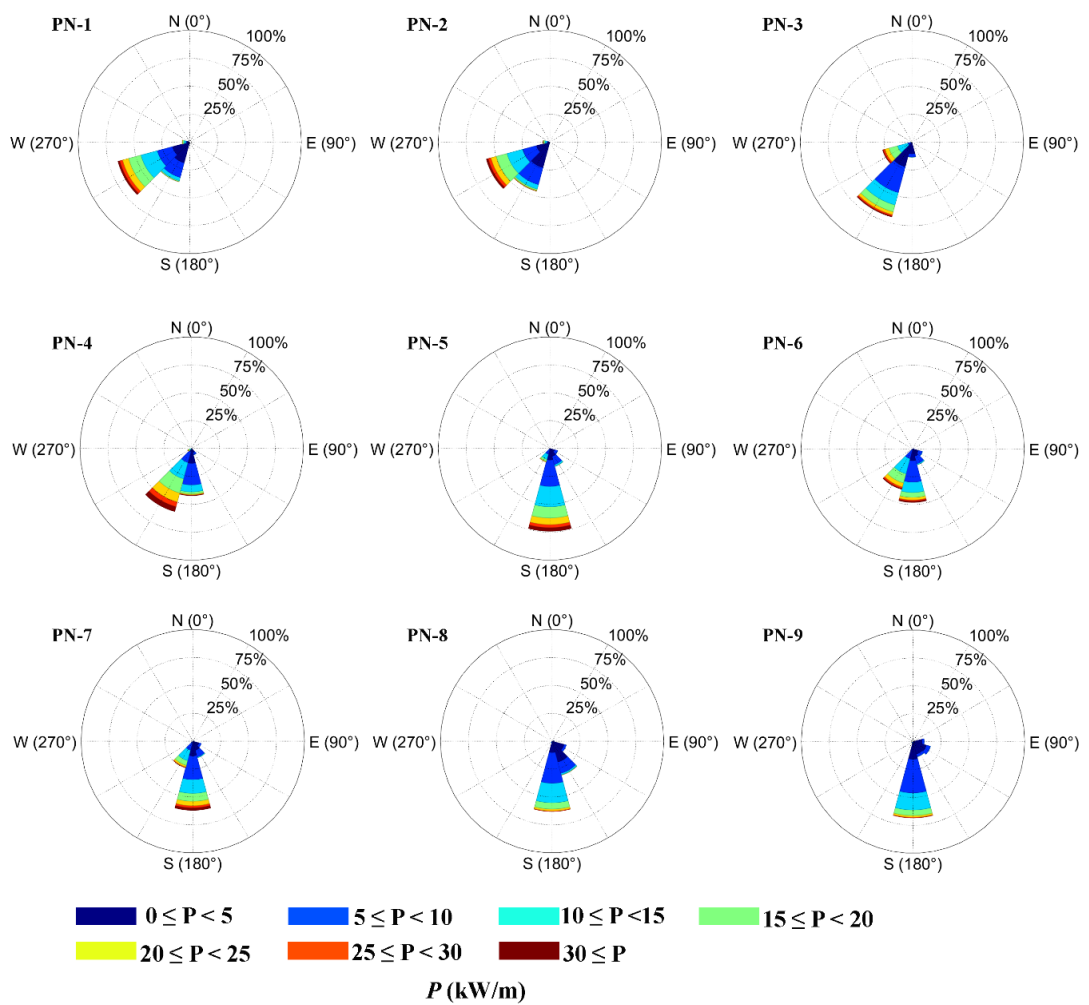


Figure 5.4: Wave power distribution at the selected nearshore locations (PN-1 to PN-9) around the south-west to south-east coastline of Sri Lanka.

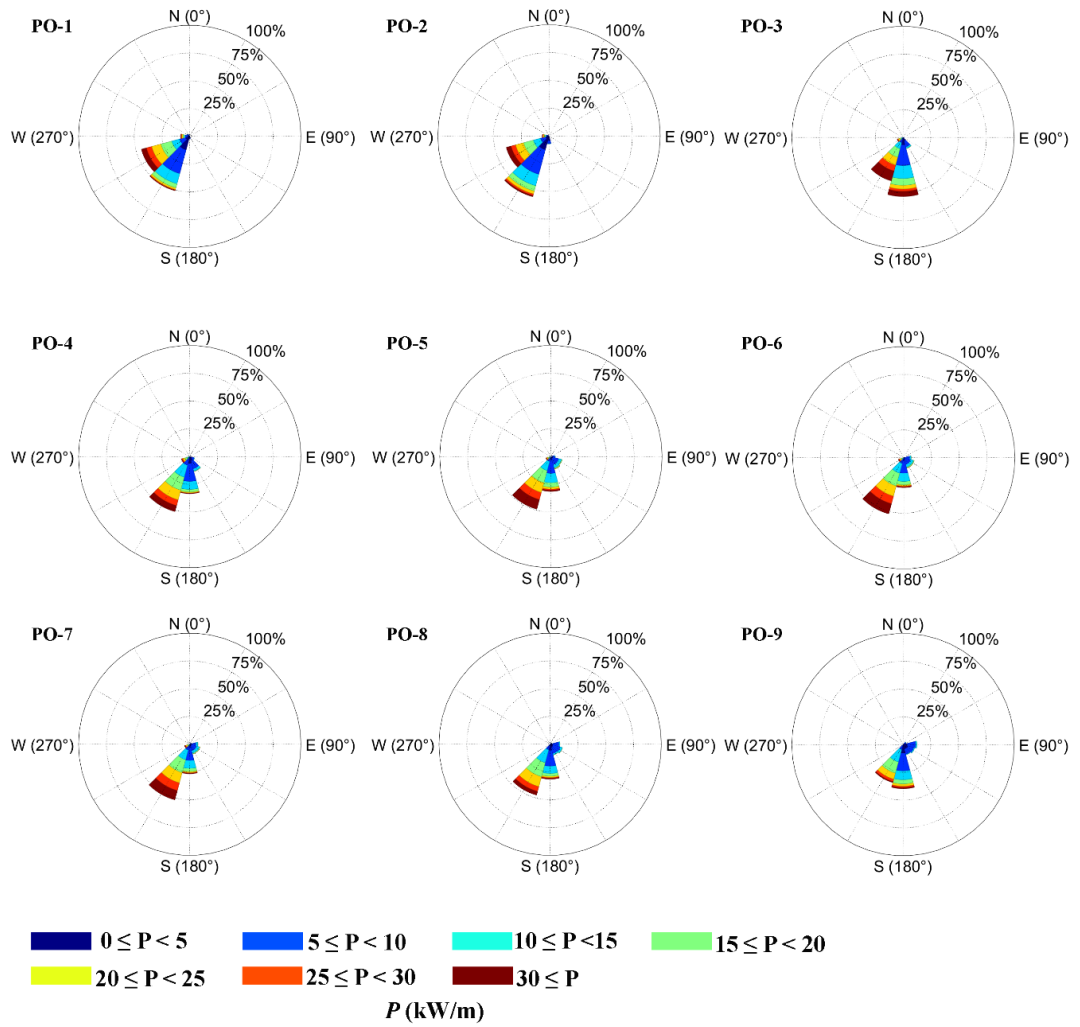


Figure 5.5: Wave power distribution at the selected offshore locations (PO-1 to PO-9) around the south-west to south-east coastline of Sri Lanka.

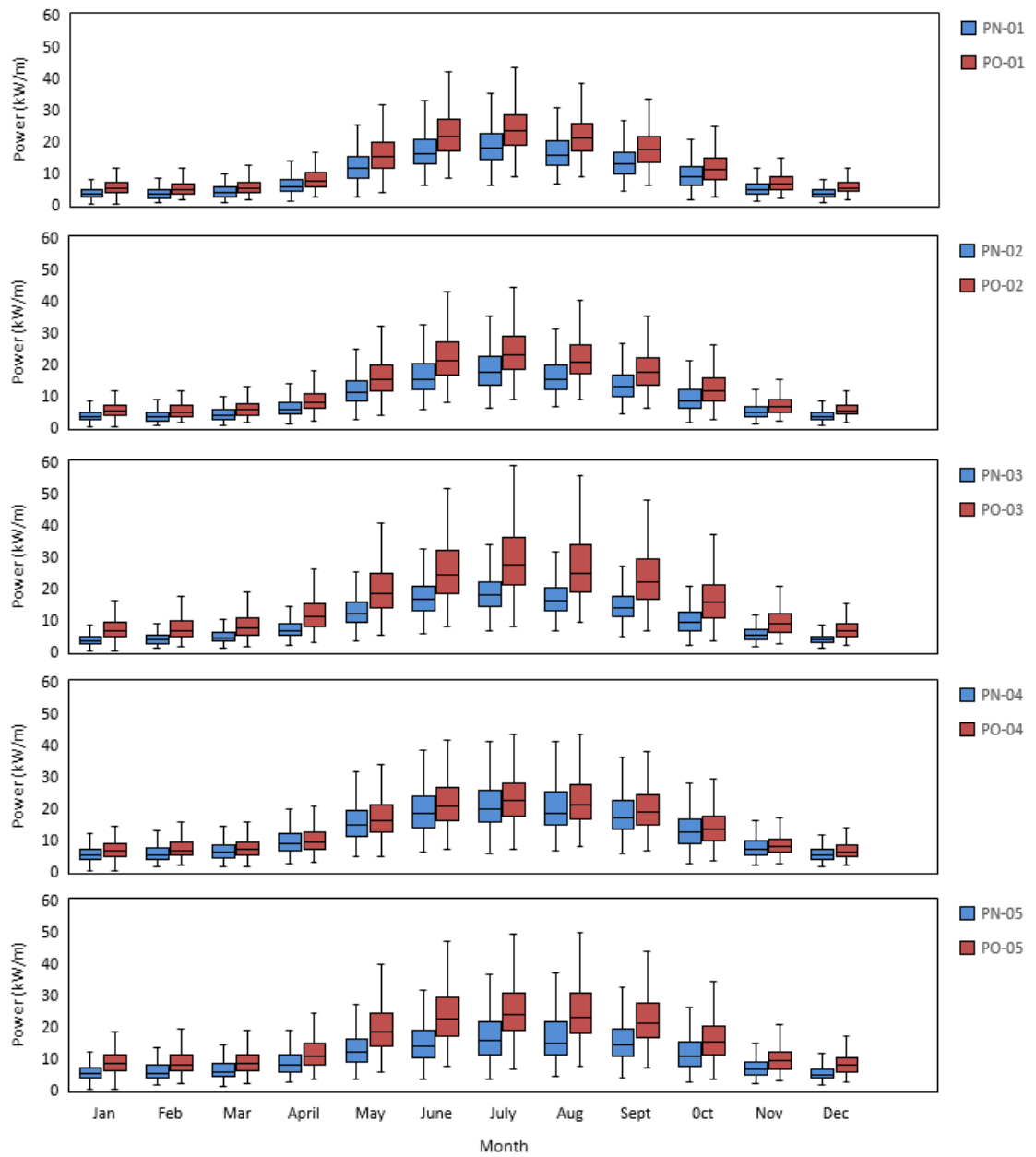


Figure 5.6: Box-Whisker plots of offshore and nearshore wave power around the south-west to south-east coastline of Sri Lanka.(for PN-01 to PN-05).



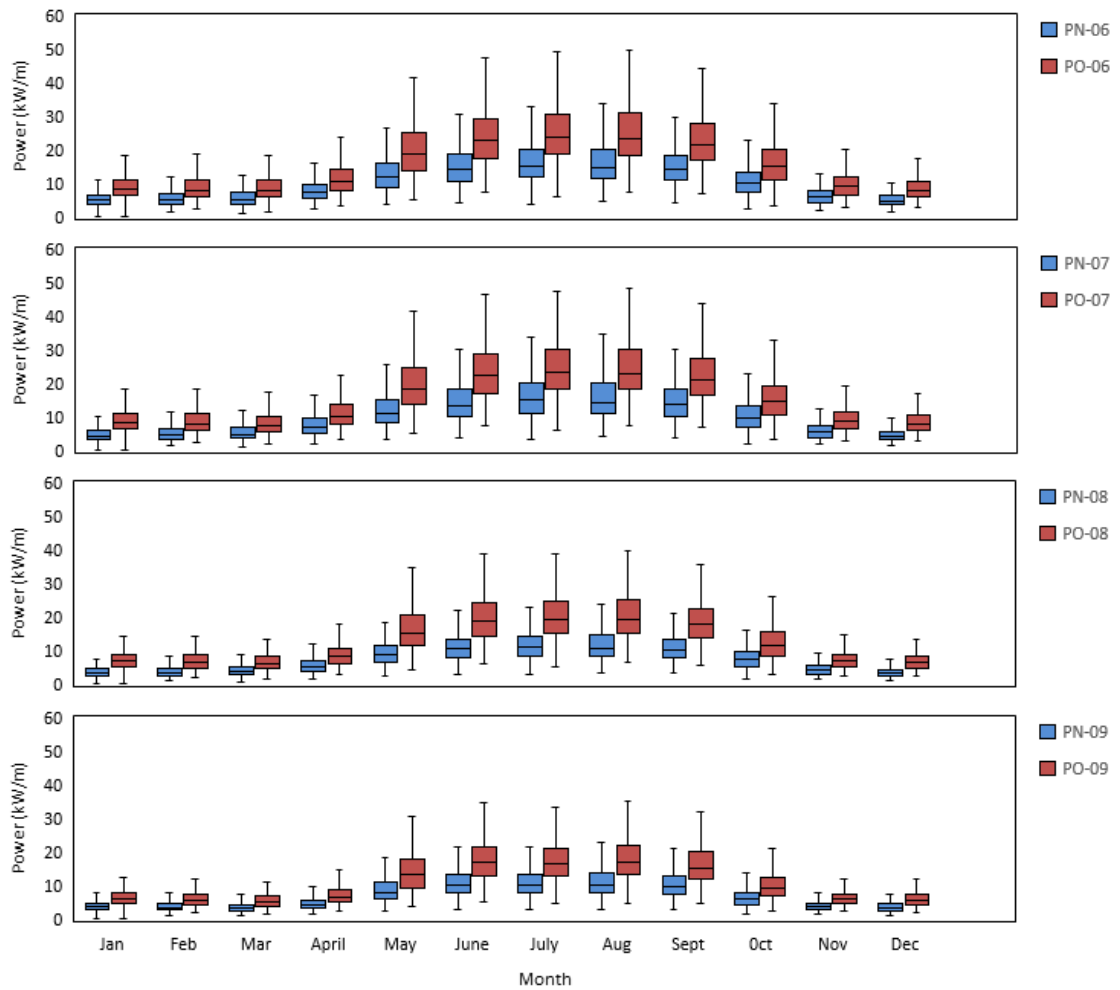


Figure 5.7: Box-Whisker plots of offshore and nearshore wave power around the south-west to south-east coastline of Sri Lanka.(for PN-06 to PN-09).

In addition to the seasonal cyclones, local climatic variabilities in the Indian Ocean such as Equatorial Indian Ocean Oscillation and the Indian Ocean Dipole (IOD) (EQUINOO) (Gadgil et al., 2004) may effects the Indian regional wave climate. Therefore, it influences the available wave power and power stability at inter-annual to decadal scale variations. To investigate wave power variability at timescales larger than the seasonal scale, annual average offshore and nearshore wave power at all selected offshore and nearshore locations were determined and evaluated (Figure 5.8).

As seen in Figure 5.8, annual average wave power remains largely steady at inter-annual to decadal timescale along the entire south-west to south-east coastline although a faint cyclic variation where the average wave power drops slightly in every 5-7 years can be seen. However, this variability could not be directly correlated to any local climatic variability in the northern Indian Ocean. It can also be seen that the trend of variability along the coast is fairly uniform. The figure also clearly reveals the change of annual average wave power from the offshore to the nearshore. At almost all points selected for this analysis, a significant reduction of annual average wave power can be seen in the nearshore, except at point PN-4 where both offshore and nearshore values differ only by 10-15%. In most other places, the reduction is in the order of 30%-50%.

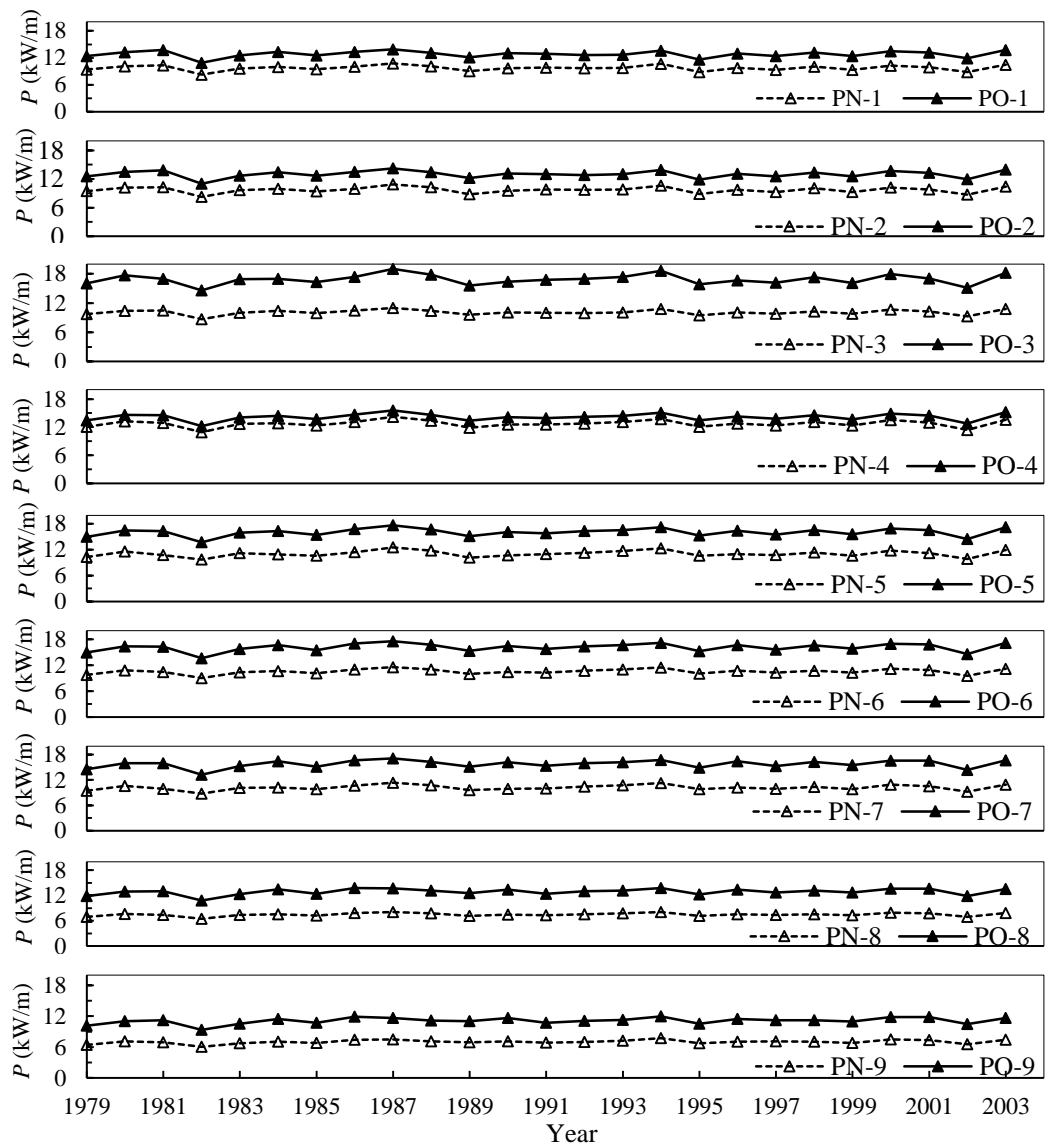


Figure 5.8: Annual average wave power at selected 18 locations for the period 1979-2003. Broken lines refer to the nearshore points while dark lines refer to the offshore points

### 5.2.3 Wave power matrix

The actual power yield from a wave energy harvesting device depends on the power matrix of that device, which can considerably vary between devices (Reeve D.E., Chen S., Pan S., Magar V., Simmonds D.J. and Zacharioudaki A., 2011). Although it is not intended to focus on a particular wave energy device, to support wave energy

developers who may be interested in wave power generation projects in Sri Lanka, the power matrices of 'available wave power' for locations all nearshore selected locations were developed (Figure 5.9 and 5.10). The wave energy yield from each bin can be determined from the product of the significant wave height and the energy period corresponding that that bin if the power rate of power generation of a given device is known. The summation of energy from all bins will then gives the total energy production.

Most of the power yield in nearshore locations varies within 1.5 m -2.0 m significant wave height region and 7 s – 10 s energy period region. Also, 30 – 45 % of the total available wave energy concentrated in this region. A similar analysis was carried out for all selected offshore locations (Figure 5.11 and 5.12).

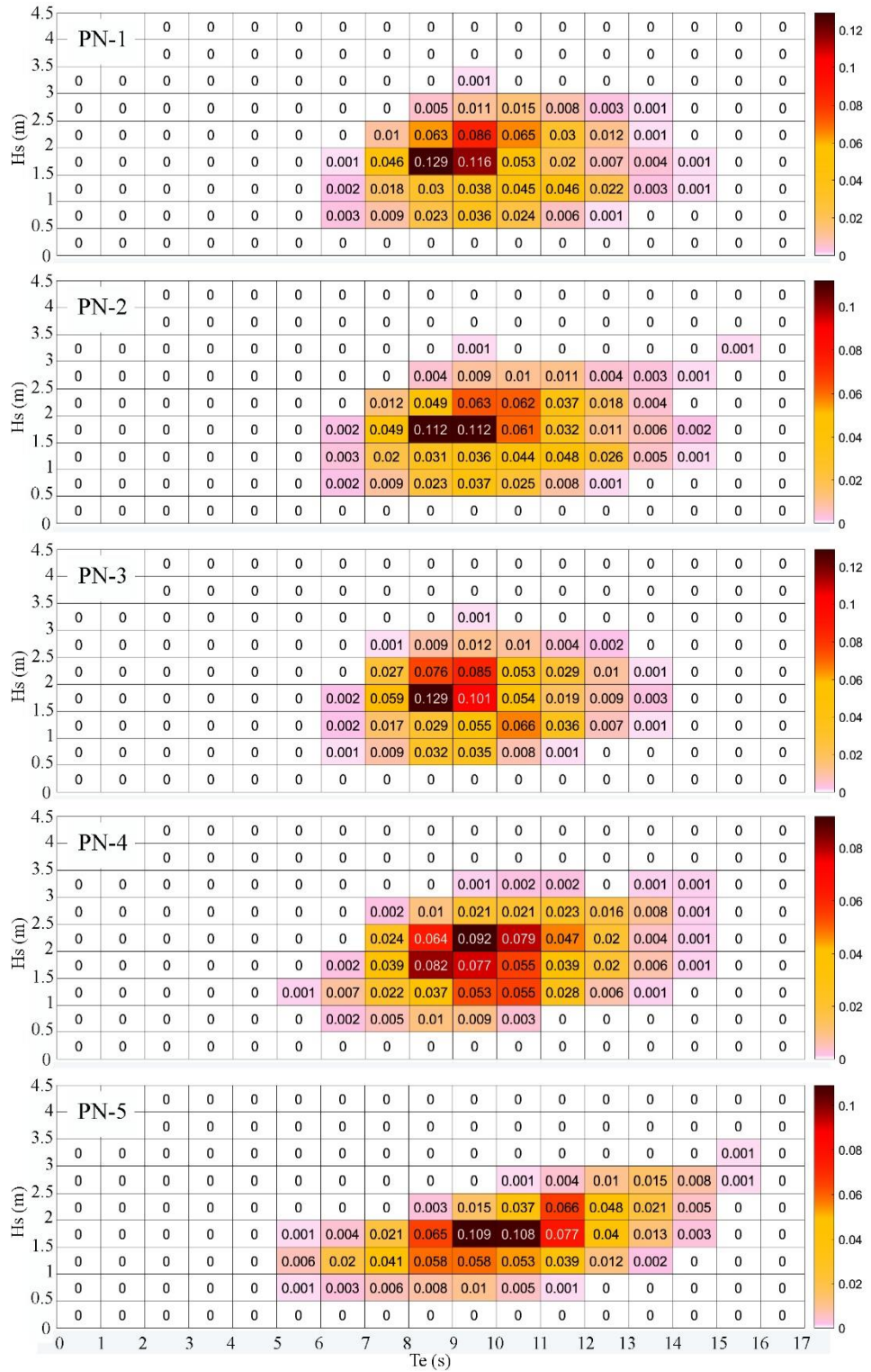


Figure 5.9: Power matrices of available wave power at locations PN-1 to PN-5. Power is given as a fraction of available power in each sea state to total power available at the selected location

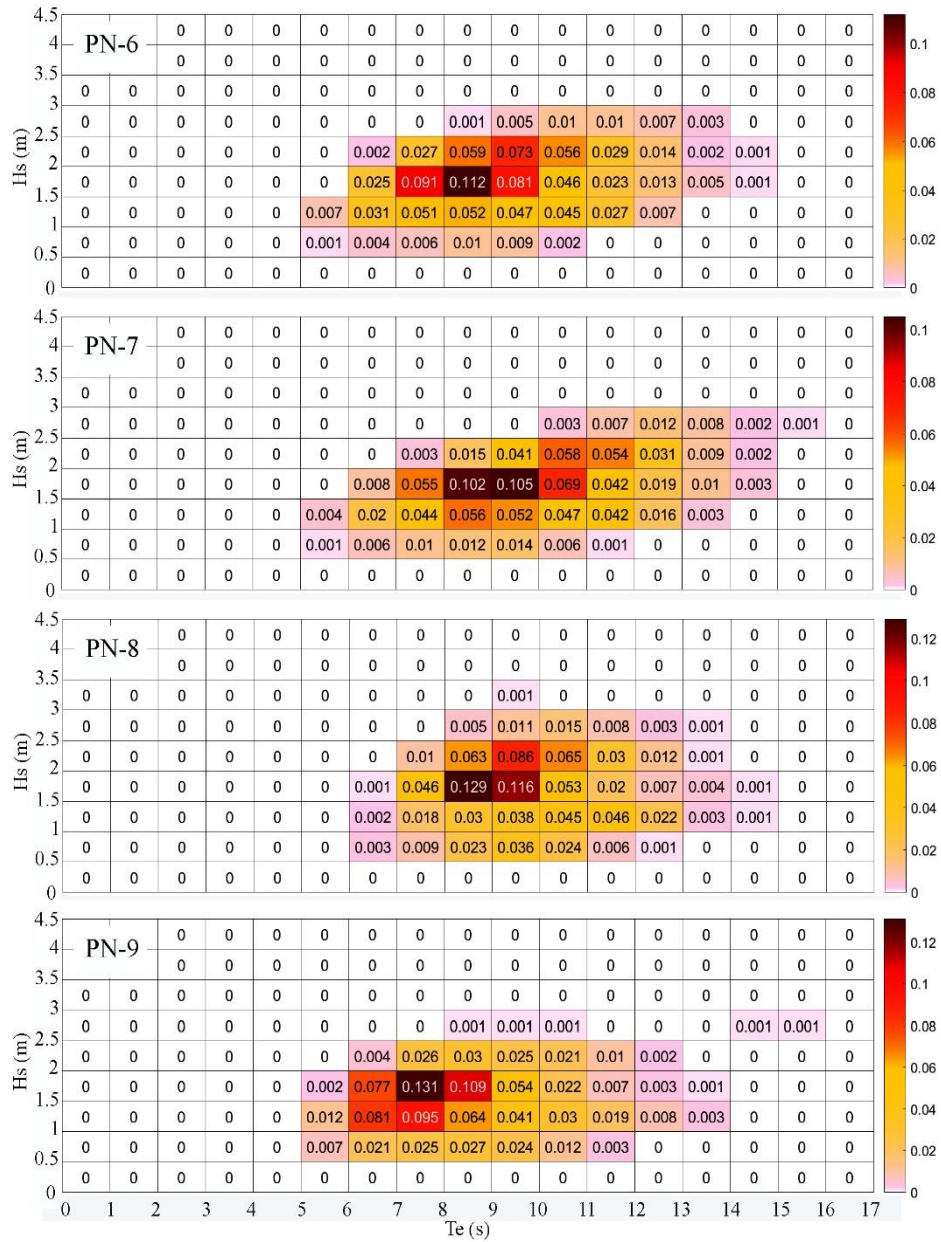


Figure 5.10: Power matrices of available wave power at locations PN-6 to PN-9. Power is given as a fraction of available power in each sea state to total power available at the selected location

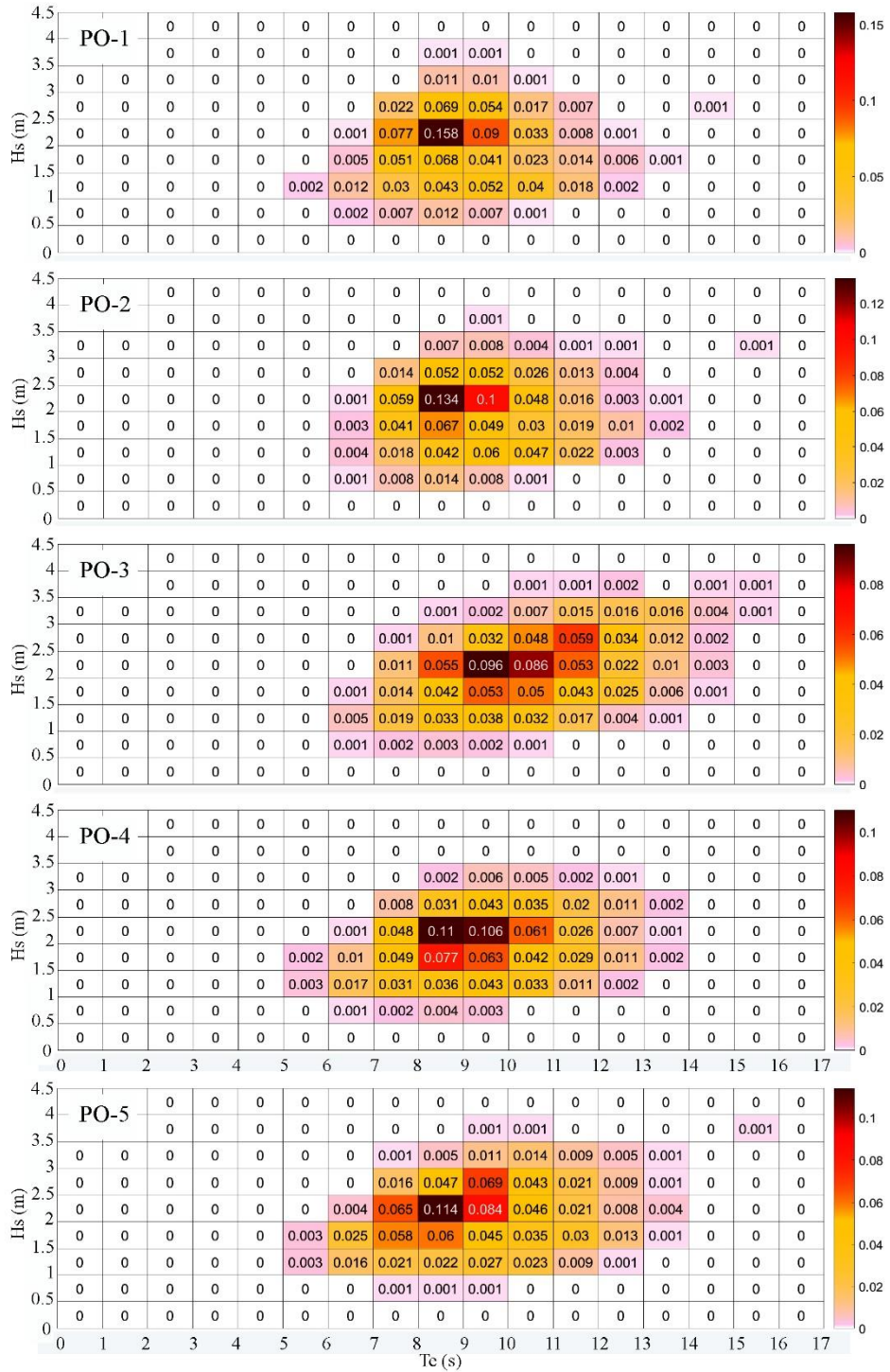


Figure 5.11: Power matrices of available wave power at locations PO-1 to PO-5. Power is given as a fraction of available power in each sea state to total power available at the selected location

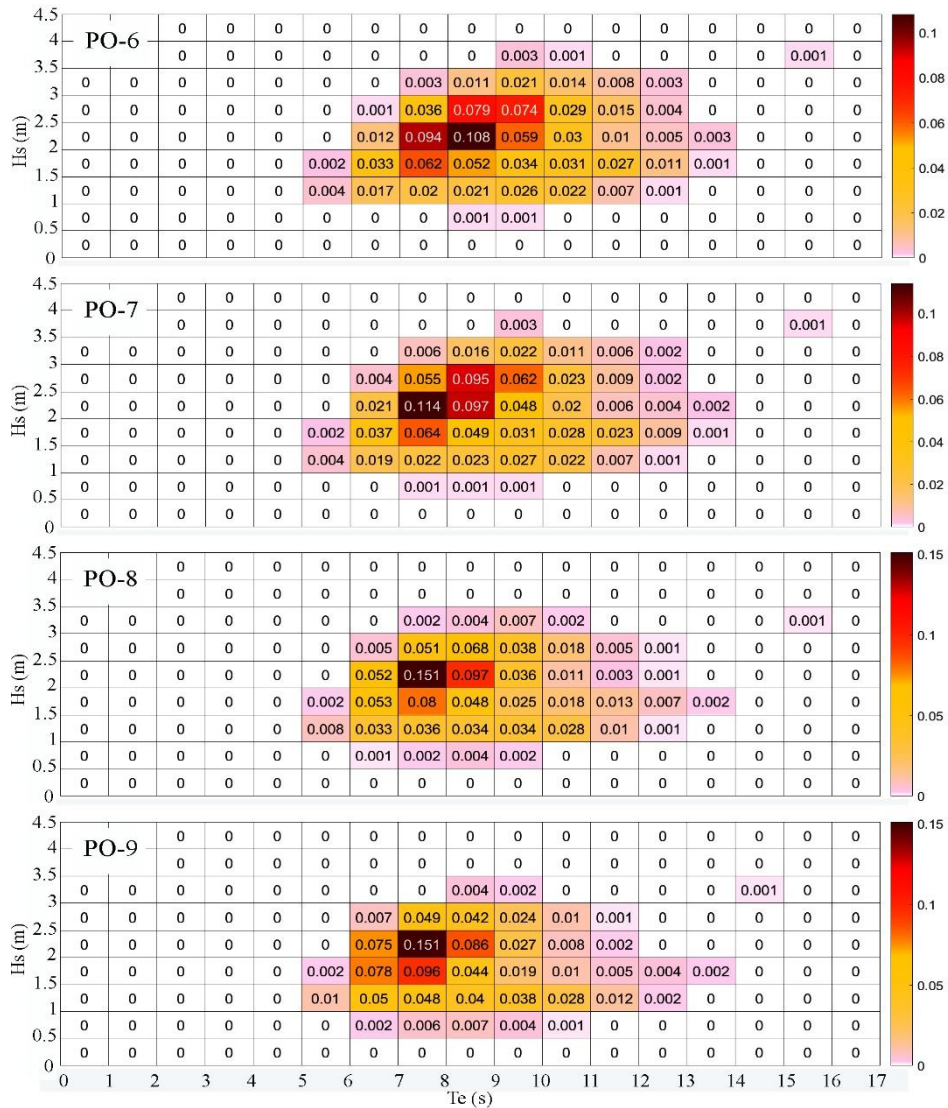


Figure 5.12: Power matrices of available wave power at locations PO-6 to PO-9. Power is given as a fraction of available power in each sea state to total power available at the selected location

### 5.2.4 A summary of available wave energy resource

A summary of the available wave power and its stability around the west to the south-east coast of Sri Lanka is given in Figure 5.13. In this figure, the radius of a circle is proportional to the average available wave power. The colour bar indicates the range of variability available wave power within the 25-year modelling period (1979 to 2003) where red indicates high variability while green indicates low variability.



It is clear that most available wave power is in the offshore of south-western and southern areas while relatively less energy is seen in the west and the south-east. As also seen in Figure 5.13, nearshore areas have a significantly low wave power. Resource variability is high in the western and southwestern coasts of Sri Lanka (both nearshore and offshore) while the resource is more stable in the south, making the south of Sri Lanka as the most suitable area for wave energy harvesting. Overall, the offshore power variability is significantly higher than that of the nearshore in all areas.

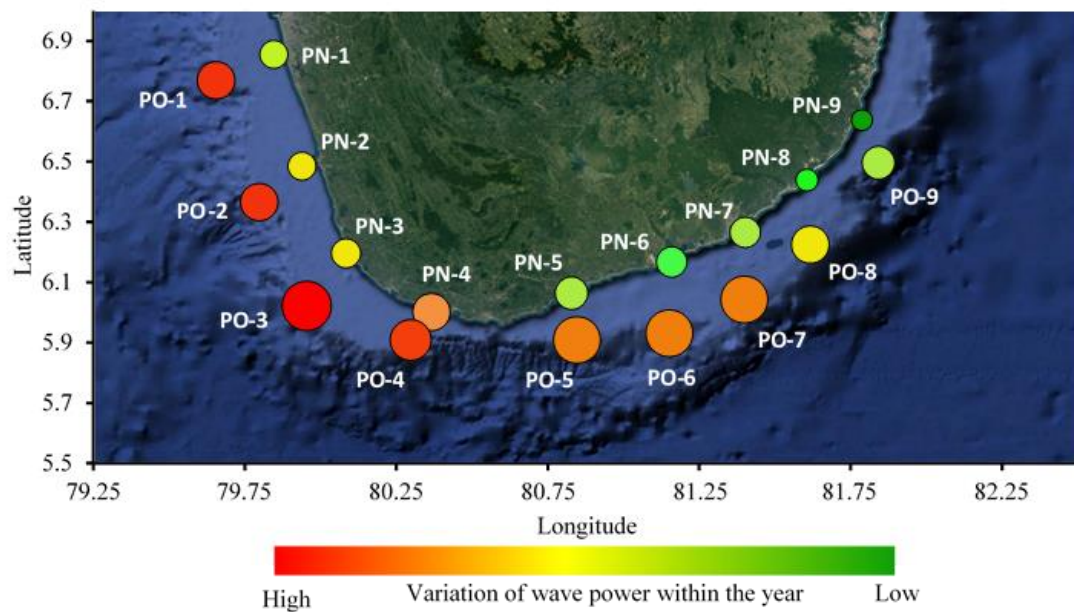


Figure 5.13: A summary of spatial variation and range of variation of wave power around south-west to south-east coast of Sri Lanka. The radius of circles proportional to the amount of average wave power. Red, yellow and green in the colour bar indicates high, average and low range of variability of wave power.

## **6.0 IMPACTS OF GLOBAL CLIMATE CHANGE ON THE OCEAN WAVE ENERGY RESOURCE**

### **6.1 Introduction**

The characterisation and assessment of the existing wave energy resource is the starting point of any wave energy harvesting project. It is well understood that the ocean wave climate and hence the available wave energy resource at any given location varies at a range of timescales from a few days to a few years, as a result of extreme events such as storms and tropical and extra-tropical cyclones, seasonal events like tropical monsoons and annual/inter-annual climatic variabilities such as North Atlantic Oscillation (NAO), Southern Oscillation (SO) and Indian Ocean Dipole (IOD) among others. Furthermore, global climate change may have the potential to impact the available wave resource at much longer timescales of several decades or longer.

Considering the necessity of investigating the sustainability of the available resources, the above studies highlight the importance of assessing climate change impacts on the future wave energy resource before embarking any future wave energy development. In the study presented in this paper, we will assess the implications of global climate change on the ocean wave energy resource around Sri Lanka, an island located in the Northern Indian Ocean with a considerable potential of wave energy due to being exposed to ocean waves transferring from the Southern Indian Ocean. We will also investigate the stability and sustainability of the wave resource in future, when compared to the present situation that prevails under the current global climate. Present and future wave data used in this study are derived from the spectral wave model SWAN, using climate information provided by a super-high-resolution GCM, MRI-AGCM3.2S (Mizuta R., Yoshimura H., and Murakami H., 2012).

### **6.2 Climate change impact on wave power variations**

As described in section 4, the validated Sri Lanka regional wave model provided wave simulations for two-time slices, representing ‘present’ and ‘future’ wave climate of the Sri Lanka region (25-years wave data for the period between 1979-2003, representing the present wave climate and between 2075-2099). The modeled future wave

projections were used to investigate climate change impacts on wave power potential of Sri Lanka.

### 6.2.1 Spatial distribution of future wave power

In Figure 6.1, the average wave power resource (averaged over 25-year period between 1979 and 2003 for the ‘present’ and between 2075 and 2099 for the ‘future’ projection) is shown to investigate the spatial distribution of average wave power around Sri Lanka. On average, 10-16 kW/m of wave power is available on the continental shelf of the south and west coasts of Sri Lanka under the current climate. In contrast, only 2-6 kW/m of wave power is available in the north and east (Figure 6.1 (a)). The average wave power under the future climate scenario (2075-2099) given in Figure 6.1 (b) shows an overall reduction of 1.5-2.5 kW/m of power in the south and west in the future. No noticeable change is seen in the north and east coastal region.

The difference between ‘future’ and ‘present’ total averaged wave power was calculated and shown in Figure 6.2 for further understanding. The difference was calculated as ‘total average wave power in future’- ‘total average wave power in present’ for the entire model domain.

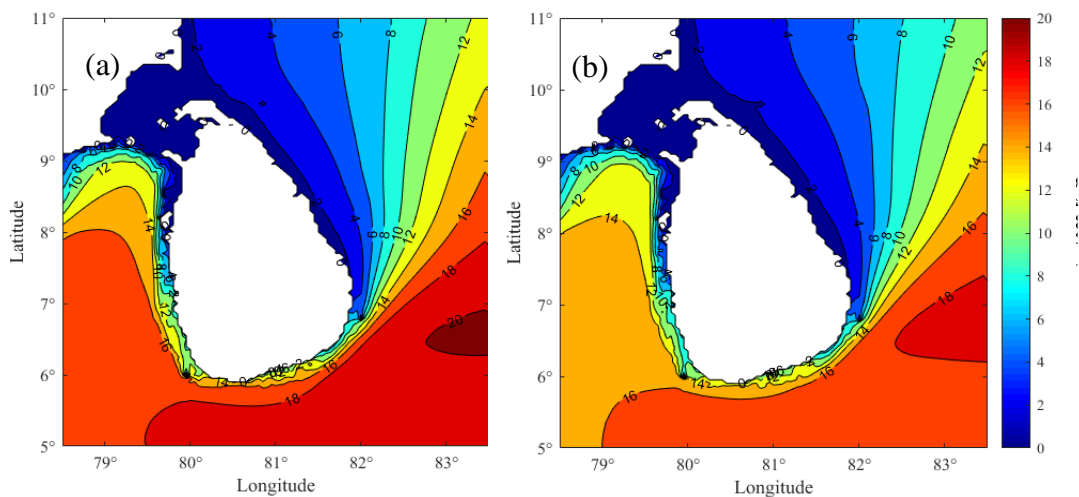


Figure 6.1: The distribution of average wave power around Sri Lanka. (a) ‘present’ 25-year simulation period from 1979 to 2003 ; and (b) ‘future’ 25-year simulation period from 2075 to 2099.

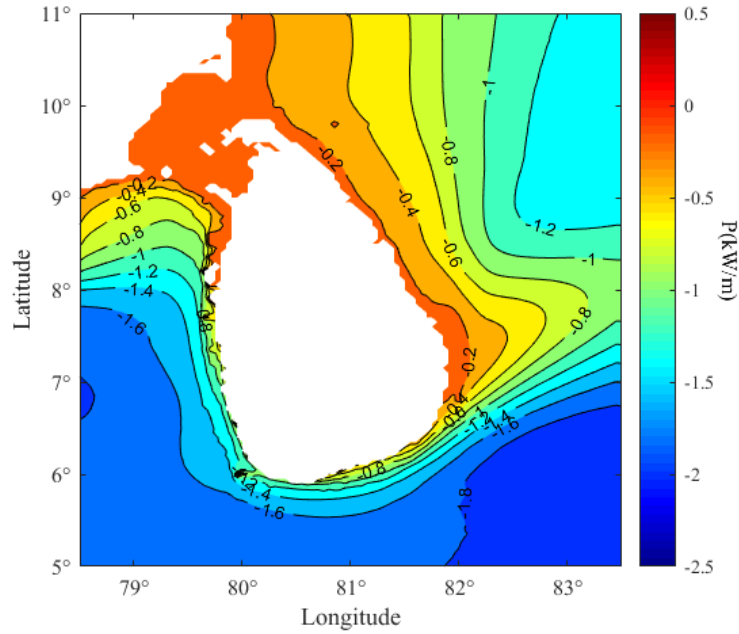


Figure 6.2: The distribution of difference between ‘future’ and ‘present’ average wave power (Future-Present) around Sri Lanka

As described under section 5, Sri Lanka is affected by tropical monsoon climate systems in the Indian Ocean which leads to a significant variation in monthly averaged wave power distributions. In Figure 6.3, the difference between ‘future’ and ‘present’ monthly averaged wave power, averaged over the 25-year simulation periods, is shown. During the non-monsoon months from October to April, the future reduction of monthly average wave power along the west and south continental shelf margin is fairly uniform along the coast and is less than 0.8 kW/m at any given location. On the other hand, wave power during the south-west tropical monsoon (May-September) is reduced by a maximum of 3.2 kW/m in future although this reduction is significantly space-dependent. The largest reduction is seen in the south-west and south-east.

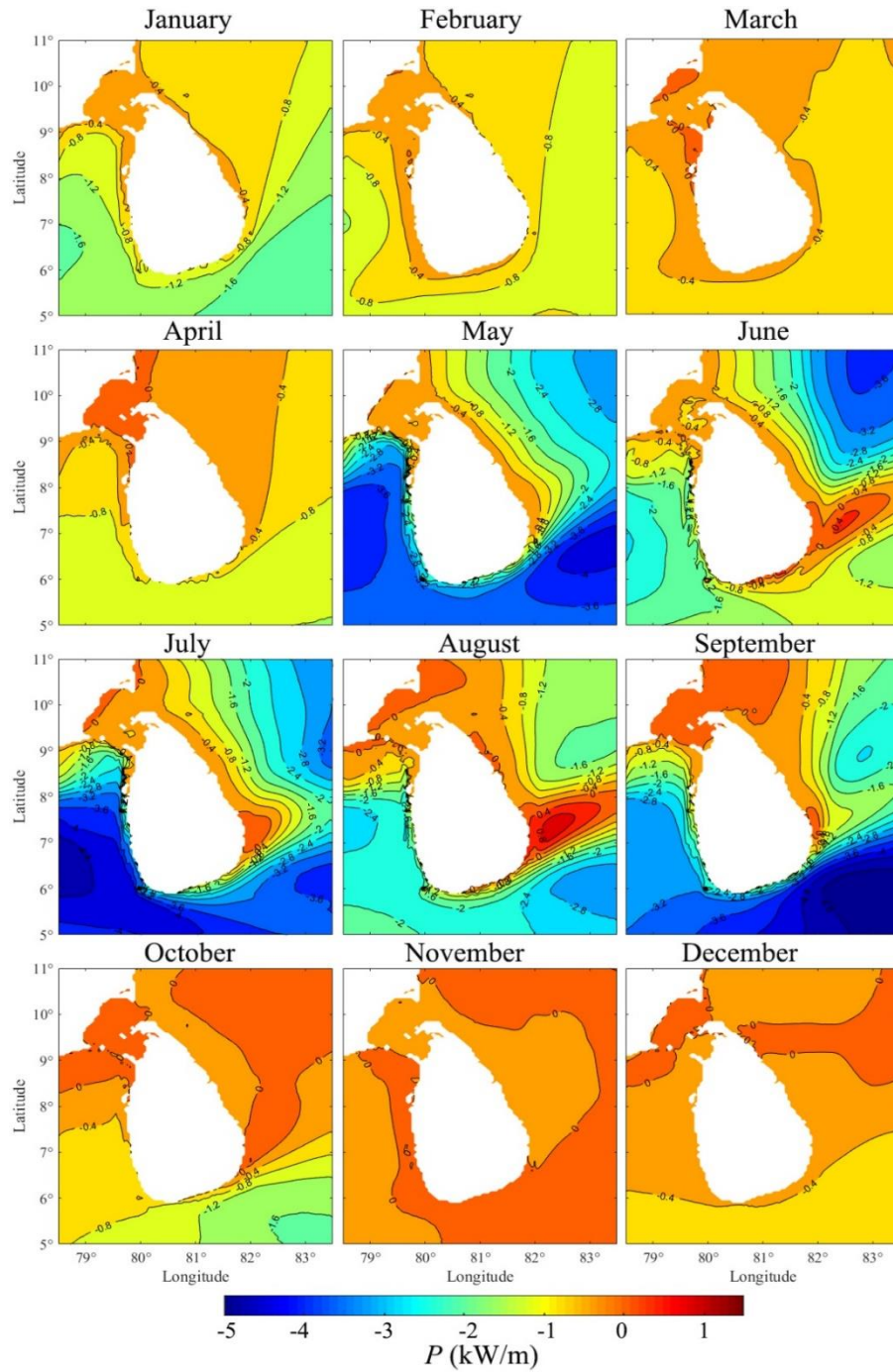


Figure 6.3: The difference between ‘future’ and ‘present’ monthly averaged wave power

Figure 6.3 reveals that according to the model simulations, the future reduction of wave power may be attributed to the change in the south-west tropical monsoon generated wave heights as a result of global climate change.

### 6.2.2 Effect of monsoon systems

Future reduction in the available wave power around Sri Lanka can be either due to change in swell conditions of the southern Indian Ocean or due to potential changes to the south-west tropical monsoon. In Figure 6.4 (a), the difference between future and present average wave power during south-west monsoon months (May-September, averaged over the 25-year period) is shown. A similar figure for the non-SW-monsoon period (October-April) is given in Figure 6.4 (b).

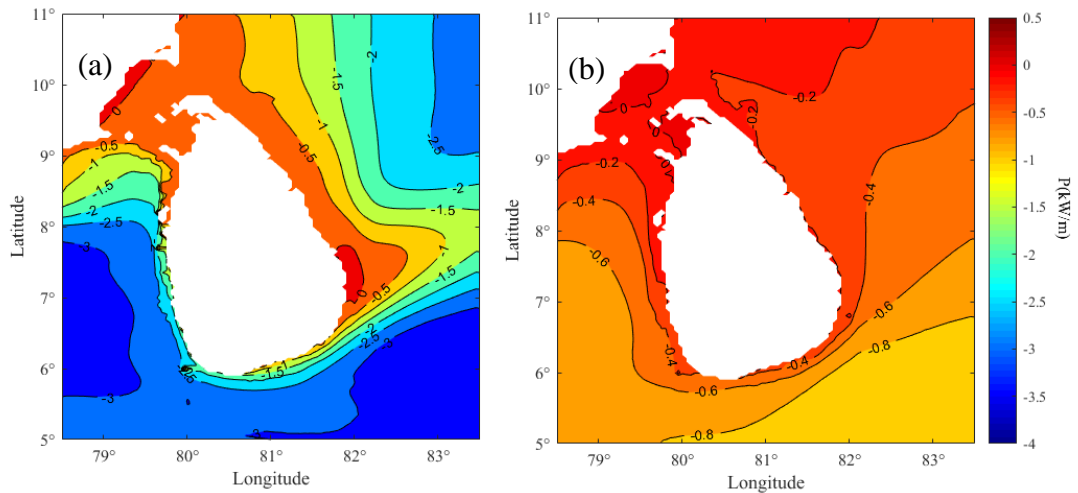


Figure 6.4: Difference between ‘future’ and ‘present’ average wave power during (a) monsoon (May-September) and (b) non-SW-monsoon (October-April) periods

The highest change is observed in the south-west as expected, where the average wave power on the continental shelf during the monsoon has reduced by around 2.5 kW/m on average in future during the south-west monsoon period. But during the rest of the year, the reduction of wave power remains around 0.6-0.8 kW/m.

This reduction of wave power can be caused by the variations of wave height or variations in wave periods or both. Therefore, similar figures were plotted for the total average difference of significant wave height and  $T_{m-10}$  as shown in Figure 6.5 and Figure 6.6.

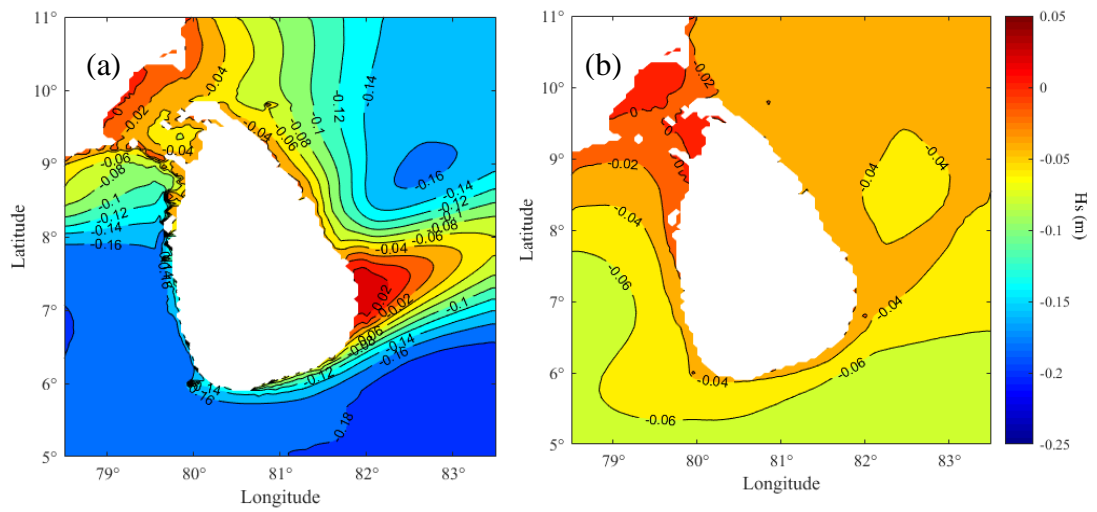


Figure 6.5: Difference between ‘future’ and ‘present’ average significant wave height during (a) monsoon (May-September) and (b) non-SW-monsoon (October-April) periods

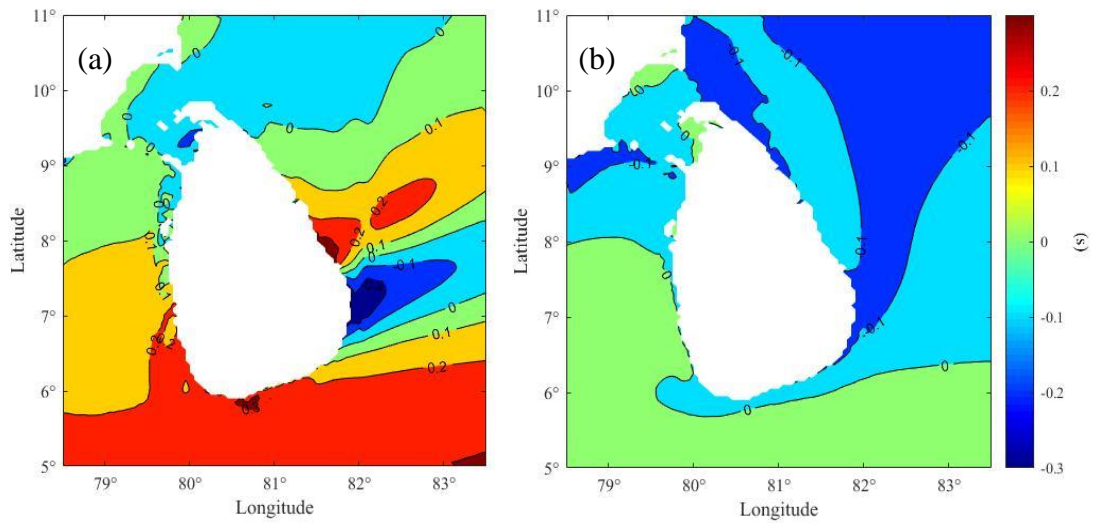


Figure 6.6: Difference between ‘future’ and ‘present’ average Tm-10 during (a) monsoon (May-September) and (b) non-SW-monsoon (October-April)

According to the Figure 6.5 and Figure 6.6, in the south-west coastal region the average significant wave height on the continental shelf during the monsoon has reduced by around 0.12 m on average in future. The reduction of the average wave height during the non-south-west monsoon period is less than 0.04m. No notable

reduction of average  $T_{m-10}$  can be seen during throughout the year and its variations are usually less than 0.2 s.

### 6.2.3 Temporal and directional wave power variations in the future

To investigate the spatial distribution of available wave power in the south and west in greater detail, ten locations, M1 to M10, along the western and southern continental shelf margin of Sri Lanka were selected (Table 6.1, Figure 6.7). The selected points are located close to the continental shelf margin and collectively cover the coast from north-west to south-east. ‘present’ and ‘future’ time series of 25-year wave simulations

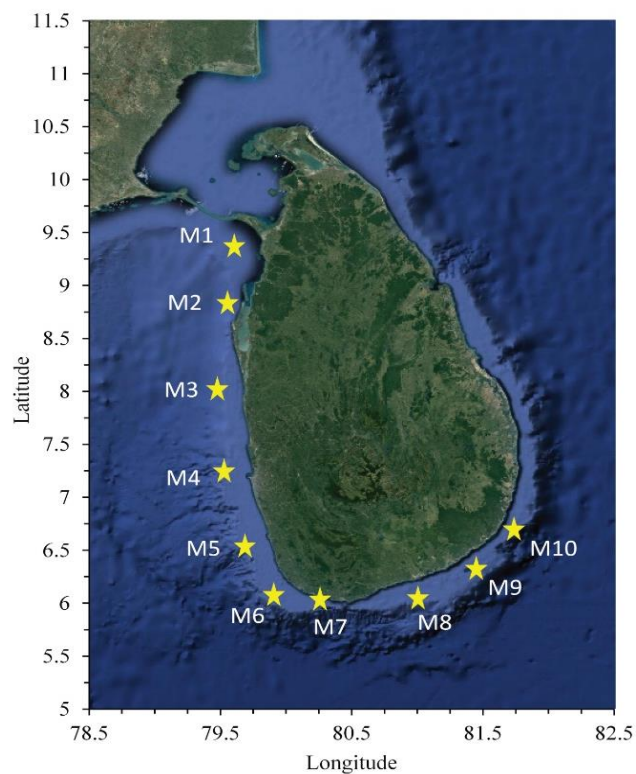


Figure 6.7: Offshore locations around the west and south coast selected

at those ten points were extracted from the simulation results for the following analysis.



Table 6.1: Coordinates and water depths of locations selected for detailed analysis of climate change impacts on the wave resource around Sri Lanka

<b>Location (Fig. 6)</b>	<b>Easting</b>	<b>Northing</b>	<b>Water depth (m)</b>
M1	79°45'00"	8°45'00"	18
M2	79°42'00"	8°18'00"	30
M3	79°36'00"	7°36'00"	100
M4	79°39'00"	6°54'00"	45
M5	79°51'00"	6°21'00"	63
M6	80°00'00"	5°57'00"	73
M7	80°21'00"	5°54'00"	58
M8	81°09'00"	5°54'00"	60
M9	81°33'00"	6°09'00"	58
M10	81°48'00"	6°27'00"	48

The annual average wave power at M1 to M10 during the ‘present’ and ‘future’ 25-year simulation periods is compared in Fig. 6.8. Averaging was done using all wave data in each year. Fig.6.8 also gives the difference between the present and future annual average wave power. M6 has the highest annual average wave power while M1 has the lowest. The low values at M1 to M3 can be attributed to the sheltered nature of the north-west coast of Sri Lanka from the southern swell approach as well as the sea waves generated by the south-west tropical monsoon. Some inter-annual variability is observed at all locations in both present and future. The highest annual variability under both present (23%) and future (24%) climates and the highest average reduction of power in future (8%) are observed at M6. The future annual average wave power is smaller than that of the present at all locations except at M1, M2 and M3 with almost no considerable change in the future.

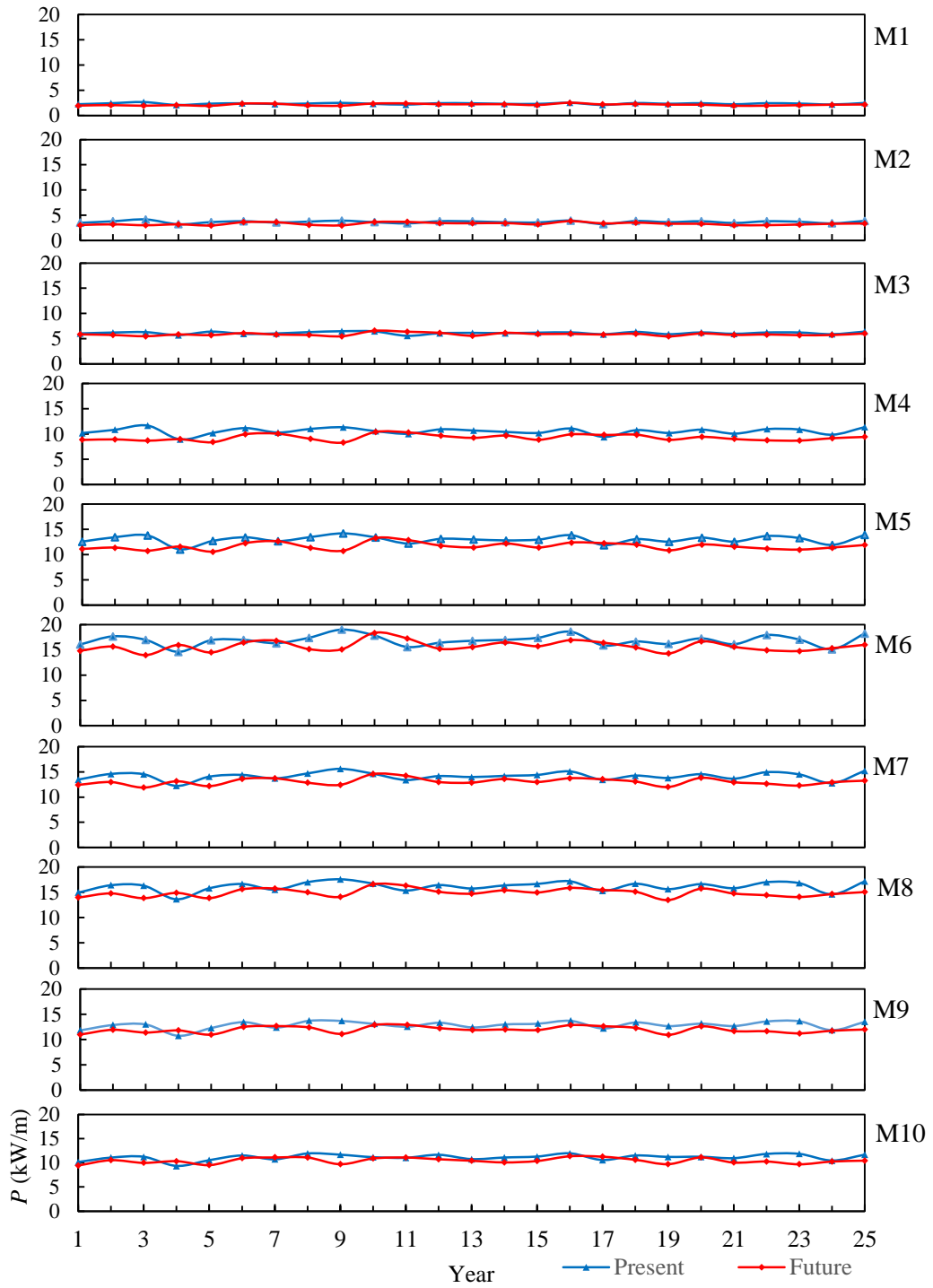


Figure 6.8: Present and future annual average wave power around Sri Lanka for M1 to M10. X-axis gives the year number, starting from the beginning of the ‘present’ and ‘future’ 25-year simulation time slices.

Although future reduction of the average available wave power and the contribution of the future changes to the south-west monsoon is apparent from the above analysis, detailed information on power variability is necessary for the planning and development of ocean wave energy harvesting projects. Box-whisker plots given in Figure 6.9 summarises the monthly variation of ‘present’ and future’ wave power at locations M1-M10 (Here, Bottom, middle and top black lines give 1st quartile, median and the last quartile. Whiskers indicate the full range of values).

These plots illustrate the monthly median, 1st and the 3rd quartiles and the range of variability for both present and future. The maximum available wave power spatially varies between 5 and 30 kW/m, lowest being at M1 (north-west) and the highest at M6 (south-west). The south-west and south of Sri Lanka from Galle to Hambantota (points M4-M8) not only has the largest available wave power but also the largest monthly variation and the highest interquartile ranges, indicating the effect of south-west monsoon on the available wave power resource.

Areas north of Colombo (Figure. 1.1) (locations M1 to M3) have the lowest available wave power, the lowest monthly variation and the lowest interquartile range. This area is sheltered from the swell approach by the protruding Puttalam lagoon and the waves are mostly locally generated. In the areas east to Hambantota (M9 & M10), some seasonal variation can be seen however, the impact of the south-west monsoon is lesser than that in the south-west. Figure 6.9 also shows that the median wave power will be smaller in future at all locations other than M1 to M3.

Incident wave approach direction, as well as the power availability, is a defining variable for the planning and development of wave energy projects. Wave power roses are given in Figure 6.10 and Figure 6.11 show the directional spread of available power percentages for ‘present’ and ‘future’ time slices respectively, for locations M1 to M10. The predominant direction is south-west at all locations while a significant proportion of power is available.

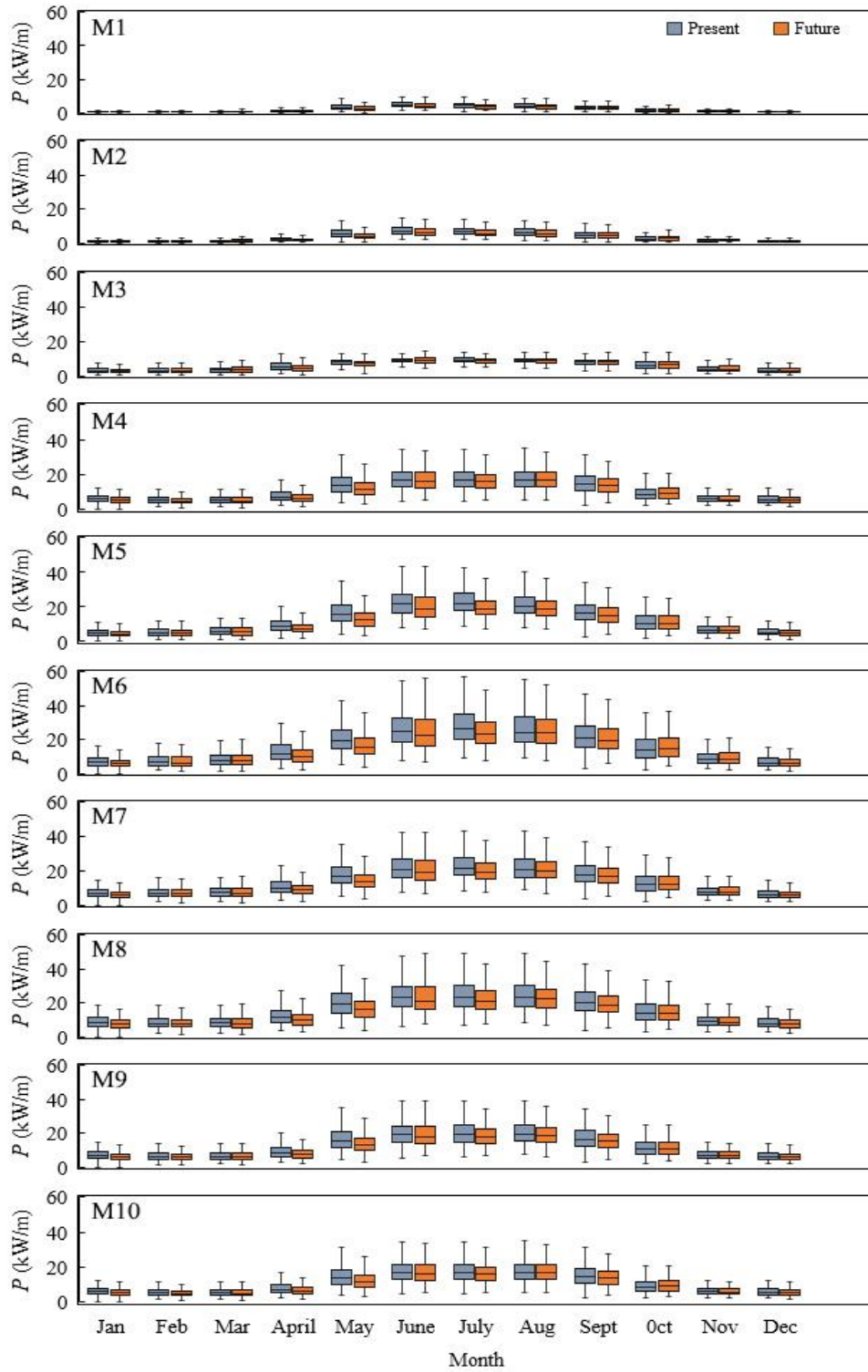


Figure 6.9: Box-Whisker diagrams of current and future wave power resource at locations M1 to M10.

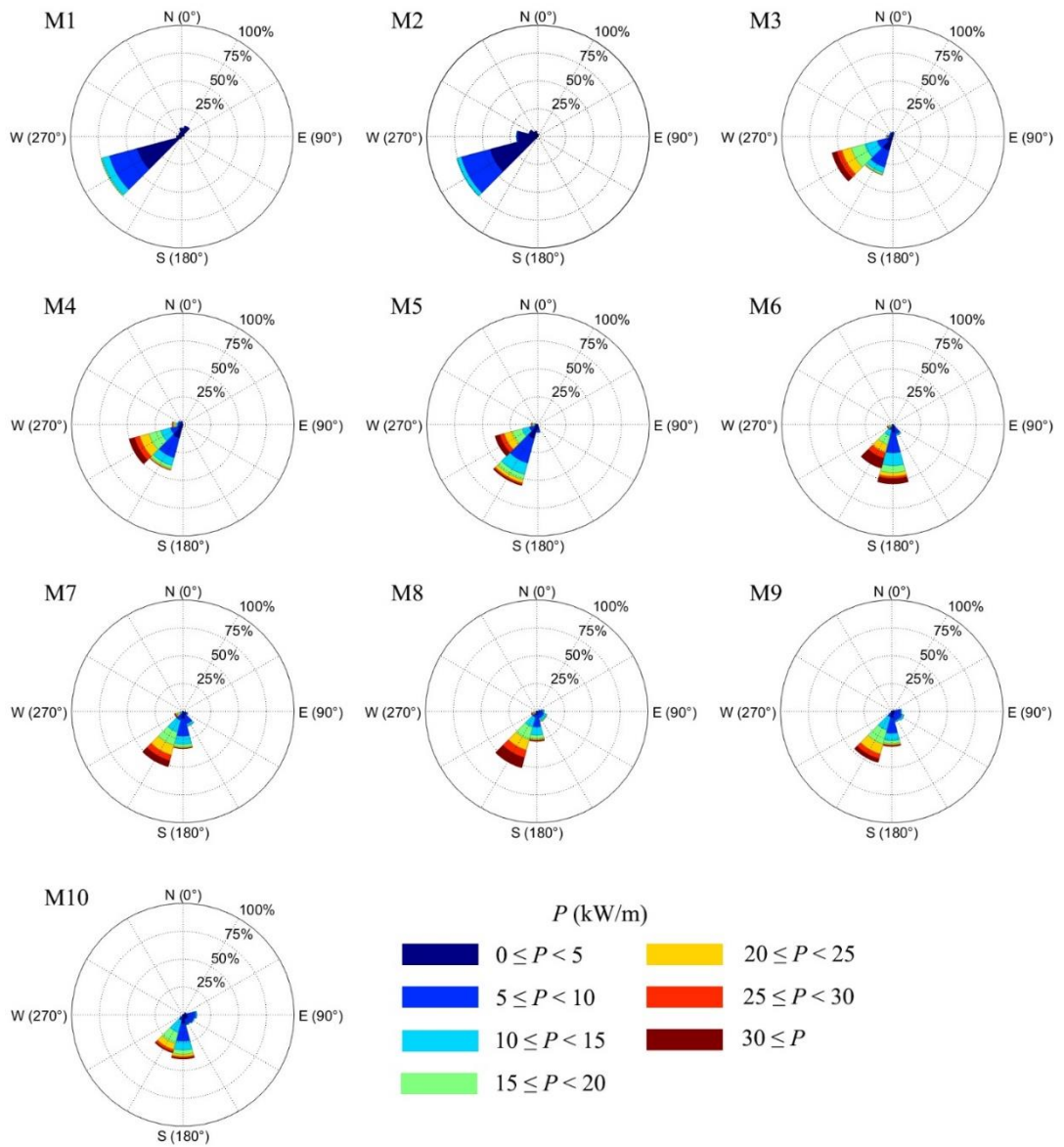


Figure 6.10: Wave power roses representing 'present' wave climate

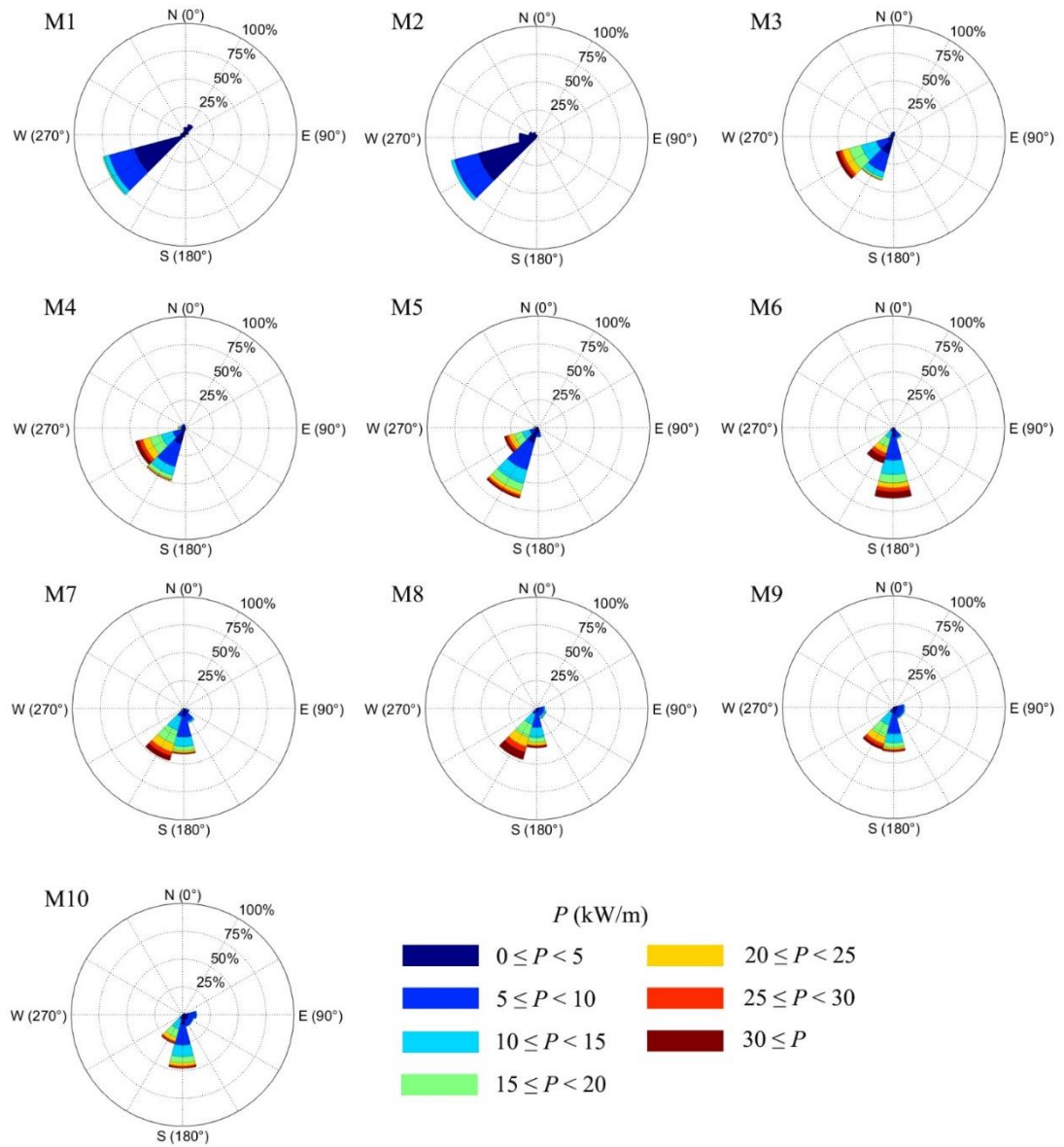


Figure 6.11: Wave power roses representing 'future' wave climate

### 6.2.4 Changes in power fraction

The available power corresponding to locally generated sea waves can be unpredictable and less stable while power available from swell waves are predictable and stable. As a result, the most desirable power capture may be from the swell waves. To study the power availability from swell and sea waves in detail and to examine the wave height range with the most power, we determined available wave power from swell and sea waves for three significant wave height bands, at locations M1 to M10. The cut-off frequency between swell and sea waves was taken as 0.125 Hz, following Sheffer et al (Sheffer H.J., Fernando K.R.M.D., Fittschen T., 1994). In Figure 6.12 present and future available wave power from sea waves ( $T_{m-10} \leq 8$  s) for 3 wave height ranges is shown as a fraction of total available power at each location. Figure 6.13 shows similar values for swell waves ( $T_{m-10} > 8$  s).

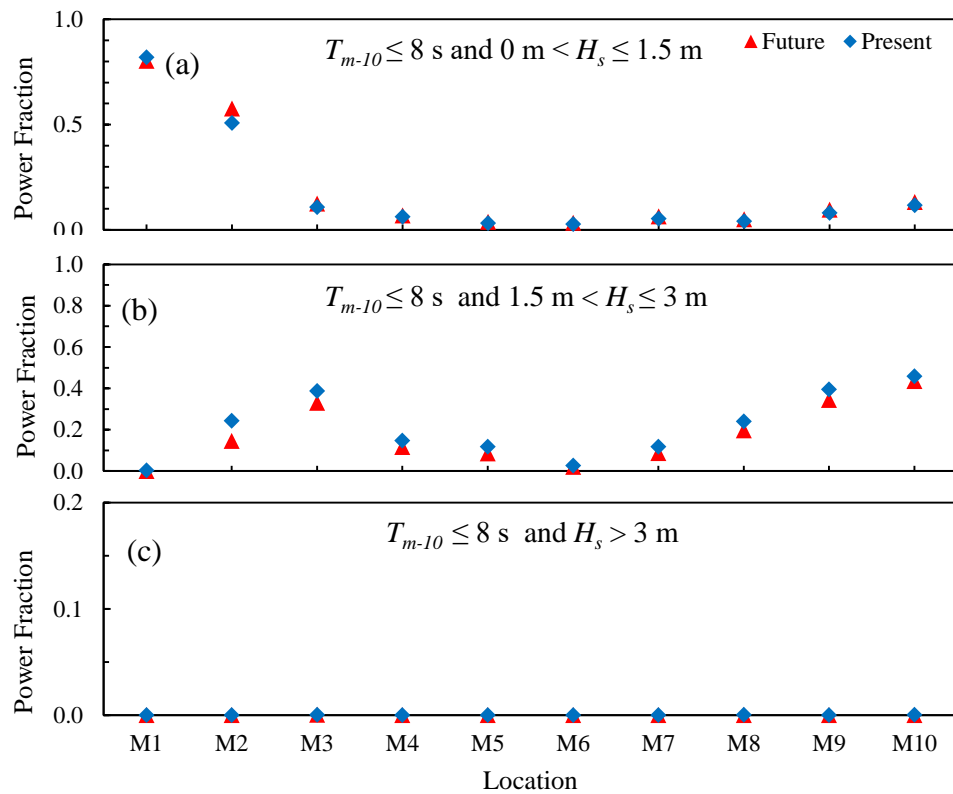


Figure 6.12: Variation of available wave power at different energy period and significant wave height classes as a fraction of total available power (for sea waves)

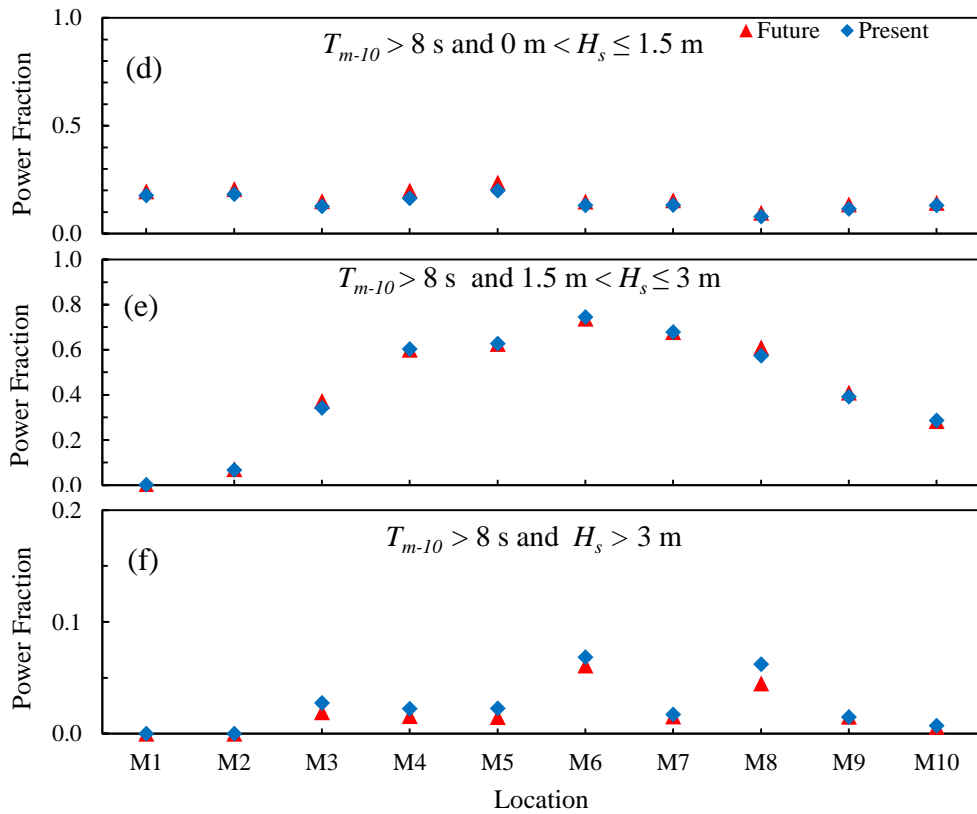


Figure 6.13: Variation of available wave power at different energy period and significant wave height classes as a fraction of total available power (for swell waves)

Figure 6.12 and Figure 6.13 lead to several observations:

- (i) Wave power from wave heights greater than 3.0 m is insignificant at all locations for both sea and swell waves;
- (ii) The largest fraction of wave power at sea wave frequencies are confined to significant wave heights between 1.5-3.0 m, except at M1 and M2 where the power fraction is larger for wave heights less than or equal to 1.5 m
- (iii) Power available from swell waves is higher than sea waves for all locations from M4 to M8
- (iv) Most power from swell waves is available from wave heights between 1.5 and 3.0 m



- (v) The fraction of swell waves at M1 and M2 is very small for all significant wave heights
- (vi) Power from sea waves of significant wave heights between 1.5 m and 3.0 m is smaller in future
- (vii) There is no notable change to power fraction from swell waves in future.

## **7.0 CONCLUSIONS**

### **7.1 Introduction**

Two sets of twenty-five years' worth projected wave data that represent the current wave climate are used in this study to investigate the spatio-temporal wave power availability around the island of Sri Lanka, located in the northern Indian Ocean. The present climate scenario covers the time period between 1979 and 2003, while the future projection covers the end of century 2075-2099-time period.

### **7.2 Wave model performance**

The high-resolution wave model used to generate wave projections is the last leg of a cascade of large-scale Indian Ocean (KU\_IO) and medium scale India regional wave models developed using SWAN spectral wave model, which has been extensively validated using numerous wave data. The high-resolution Sri Lanka wave model outputs provided the opportunity to investigate the current wave energy resource around Sri Lanka in details, which will provide essential scientific inputs for decision making and planning relating to site and device selection of future wave energy developments. Wind outputs from the MRI-AGCM3.2S, were used as the input data in this study to investigate the implications of global climate change on the available wave power around Sri Lanka.

The model performance was reasonable based on the model validation. Even during the south-west monsoon season where more energetic waves are occurred due to local wind, the modelled wave heights are matching with the measured data at validation points.

### **7.3 Wave power potential**

The results reveal that the seas surrounding south-west to south east coasts of Sri Lanka have a substantial wave power availability (10-20 kW/m on average) all throughout the year, comparable to or exceeding wave power resource identified in many countries in the world. The wave climate in this region area is characterised by long distance swell waves approaching from the south and south-west directions thus making it suitable for energy harvesting.

Although the entire south-west to south-east coast is found to have high wave power, some spatial variations can be seen. South-western region found to have higher wave power than the southern and south-eastern regions.

In addition, nearshore areas seem to have 20-50% less wave power than that at the corresponding offshore region.

#### **7.4 Temporal variations of wave power**

During the south-west monsoon season between the months of May and September, the local wave climate is dominated by the monsoon winds, and hence available wave power is strongly modulated by the monsoon wind generated sea waves.

As a result, wave power variability contains a strong seasonal signal where higher power (20-30 kW/m on average) is available from May to September. Although most of this additional power available during monsoons may be resulting from frequencies that are not entirely suitable for harvesting, the feasible range of frequencies can be device-specific.

The inter-annual to decadal scale available wave power at all locations is mostly stable although a weak cyclic signature can be seen. However, this signal could not be correlated to any regional climatic variations operating in the equatorial Indian Ocean.

#### **7.5 Climate change impact on wave energy resource**

Under the 'future' climate, the available wave power along this coastline reduces by around 1.5-2.5 kW/m, which can be considerable. Future change to the tropical south-west monsoon as a result of global climate change is found to be the cause of this reduction

The inter-annual variability of annual average wave power reduces in future. However, the reduction will be less than 10% at any given location. Although a small reduction in wave power resource as a result of future climate change is found in the most resourceful south-west and south coasts of Sri Lanka, annual average wave over time is very stable.

Potential future wave energy developments in Sri Lanka should consider the seasonal and inter-annual variability of annual average wave power under both present and future climates. The very significant spatial variability of available power should also be taken into account.

## REFERENCES

- A. John, Church, U Peter. Clark. (2013). *Climate change*. National Hurricane Center.
- Aboobacker V.M. (2017). Wave energy resource assessment for eastern Bay of Bengal and Malacca Strait. *Renewable Energy*, 14 (PA), 72-84.
- Amarasekera H.W.K.M., Abeynayake P.A.G.S., Fernando, M.A.R.M., Atputharajah A., Uyanwaththa, D.M.A.R., Gunawardena S.D.G.S.P. (2014). A feasibility study on ocean wave power generation for the southern coast of Sri Lanka: Electrical feasibility. *International Journal of Distributed Energy Resources and Smart Grids*, 10(2), 79-93.
- Anjali M., Nair and Kumar V. S. (2017). Wave spectral shapes in the coastal waters based on measured data off Karwar on the western coast of India. *Ocean Science*, 13, 365–378.
- Anoop, T.R., Kumar, V.S., Shanas, P.R. and Johnson, G. (2015). Surface wave climatology and its variability in the North Indian Ocean based on ERA Interim Reanalysis. *Atmospheric and Oceanic Technology*, 1372-1384.
- Bhaskaran, P.K., Gupta, N. and Dash, Mihir,. (2014). Wind-wave climate projections in the Indian Ocean from satellite observations. *Journal of Marine Science Research Development*, s11.
- Booij N., Ris R.C., Holthuijsen L.H., . (1999). A third-generation wave model for coastal regions. *JOURNAL OF GEOPHYSICAL RESEARCH*, 104, 1649-1666.
- Chamara R.N., Vithana H.P.V. (2018). Wave energy resource assessment for the southern coast of Sri Lanka. *6th International Symposium on Advances in Civil and Environmental Engineering*. Kuala Lumpur.
- Charles E., Idie R.D., Deleclus P., Deque. M., Le Cozannet G. (2012). Climate change impact on waves in the Bay of Biscay, France. *Ocean Dynamics*, 831-848.
- Cornett, A. (2008). A Global Wave Energy Resource Assessment. *Conference Paper in Sea Technology*.
- Department, C. C. (1997). *Coastal Zone Management Plan, Sri Lanka*. Coast Conservation Department.
- Folley M., Whittaker T.J.T. (2009). Analysis of the nearshore wave resource. *Renewable Energy*, 34, 1709-1715.
- Gadgil S., Vinayachandran P. N., Francis P. A., and Gadgil S. (2004). Extremes of the Indian summer monsoon rainfall, ENSO and equatorial Indian Ocean oscillation. *GEOPHYSICAL RESEARCH LETTERS*, 31, L12213.
- Ghosh S., Misra C. (2010). Assessing Hydrological Impacts of Climate Change: Modeling Techniques and Challenges. *The Open Hydrology Journal*, 115-121.
- Gonçalves M., Martinho P., Soares C.G. (2014). Assessment of wave energy in the Canary Islands. *Renewable Energy*, 774-784.

- Gunaratne P.P., Ranasinghe D.P.L., Sugandika T.A.N. . (2011). Assessment of Nearshore Wave Climate off the Southern Coast of Sri Lanka. *ENGINEER*, 33-42.
- Harrison G.P. and Wallace A.R. (2005). Sensitivity of Wave Energy to Climate Change. *IEEE Transactions on Energy Conversion*, 870-877.
- Hasselmann, H. and Hasselmann, K. (1985). Computations and Parameterizations of the Nonlinear Energy Transfer in a Gravity-Wave Spectrum. Part II: Parameterizations of the Nonlinear Energy Transfer for Application in Wave Models. *Physical Oceanography* , 1378-1391.
- Hemer, M.A., Fan, Y., Mori, N., Semedo, A. and Wang, X.L. (2013). Projected change in wave climate from a multi model ensemble. *Nature Climate Change*, 471-476.
- Hibbard K.A., Meehl G.A., Cox P.M., Friedlingstein P. (2007). A strategy for climate change stabilization experiments. *Earth and Space Science*, 88(20), 88:217–221.
- Hughes M.G. and Heap A.D. , (2010). National scale wave energy resource assessment in Australia. *Renewable Energy*, 35, 1783-1791.
- Iglesias G. and Carballo R. (2010). Wave energy and nearshore hotspots: The case study of the SE Bay of Biscay. *Renewable Energy*, 11 (35), 2490-2500.
- Iglesias G., Lopez M., Carballo R., Castro A., and Fraguera J.A. . ( 2009). Wave energy potential in Galicia (NW Spain). *Renewable Energy*, 2323-2333.
- Kamranzad B, Mori N. (2019). Future wind and wave climate projections in the Indian Ocean based on a super-high-resolution MRI-AGCM3.2S model projection. *Climate Dynamics*, 53(3-4), 2391–2410.
- Kamranzad B. ,Etemad-shahidi A., Chegin V. (2013). Assessment of wave energy variation in the Persian Gulf. *Ocean Engineering*, 72-80.
- Kamranzad B., Shahidi A. E., Chegini V. (2016). Sustainability of wave energy resources in southern Caspian Sea. *Energy*, 549-559.
- Kamranzad B., Shahidi A. E., Chegini V., Bakhtiary A. Y. (2015). Climate change impact on wave energy in the Persian Gulf. *Ocean Dynamics*.
- Komen, G.J., Hasselmann, S., Hasselmann, K., (1984). On the Existence of a Fully Developed Wind-Sea Spectrum. *Journal of Physical Oceanography*, 14(8), 1271-1285.
- Leijon, M., Bernhoff, H., Berg, M., Ågren, O. (2003). Economical considerations of renewable electric energy production-especially development of wave energy. *Renewable Energy*, 8, 1201–1209.
- Liang B., Fan F., Yin Z., Shi H., Lee D. (2013). Numerical modelling of the nearshore wave energy resources of Shandong. *Renewable Energy*, 330-338.
- Liberti L., Carillo A., Sannino G. (2013). Wave energy resource assessment in the Mediterranean, the Italian perspective. *Renewable Energy*, 938-949.

- Luo Y., Wang D., Gamage T.P., Zhou F., Widanage C.M. and Liu T. (2018). Wind and wave dataset for Matara Sri Lanka. *Earth Systems Science Data*, 131-138.
- Mackay E.B.L, Bahaj A.S. and Challenor P.G. (2010). Uncertainty in wave resource assessment. Part 1: Historic data. *Renewable Energy*, 1792-1808.
- Mackay, Edward B.L., Bahaj, AbuBakr S., Challenor, and Peter G. (2010). Uncertainty in wave energy resource assessment. Part 1: Historic data. *Renewable Energy*, 1792-1808.
- MARINET. (2015). *A report on 'Standards for wave data analysis, archival and presentation*.
- Mirzaei A., Tangang F, Juneng L. (2016). Wave energy potential along the east coast of Peninsular Malaysia. *Energy*, 722-734.
- Mizuta R., Yoshimura H., and Murakami H.,. (2012). Climate simulations using MRI-AGCM with 20-km grid. *Journal of the Meteorological Society of Japan*, 90A, 235-260.
- Neill N.P., Vogler A., Goward-Brown A.J., Baston S., Gillibrand P.A., Walkdon S., Woolf, D.K. (2017). The wave and tidal resource of Scotland. *Renewable Energy*, 114, 3-17.
- Portilla J, Sosa J, Cavaleri L. . (2013). Wave energy resources: wave climate and exploitation. . *Renew Energy* 2013;57:594e605., 57, 594-605.
- Reeve D.E., Chen S., Pan S., Magar V., Simmonds D.J. and Zacharioudaki A.,. (2011). An investigation of the impacts of climate change on wave energy generation: The Wave Hub, Cornwall, UK. *Renewable Energy*, 2404-2413.
- S.K. Dube, EIndu Jain, A.D. Rao, T.S. Murty`. (2009). Storm surge modelling for the Bay of Bengal and Arabian Sea. *Natural Hazards*, 3-27.
- Sanil K. V., Anoop T. R., . (2015). Wave energy resource assessment for the Indian shelf seas. *Renewable Energy*, 76, 2012-2019.
- Sheffer H.J., Fernando K.R.M.D., Fittschen T. (1994). *CCD-GTZ Directional wave climate study South-west coast of Sri Lanka, Report on the wave measurements off Galle*. Colombo.
- Team, S. (2017). *SWAN scientific and technical documentation*. Delft University of Technology.
- Thevasiyani T., Perera K. (2014). Statistical analysis of extreme ocean waves in Galle, Sri Lanka. *Weather and Climate Extremes*, 40-47.
- Thomas J., Barve K.H., Dwarakish G S., Ranganath L. R. (2015). A Review on Assessment of Wave Energy Potential. *National Conference on Futuristic Technology in Civil Engineering for Sustainable Development* (pp. 178-185). Department of Civil Engineering, SJBIT .
- Weatherall P., Marks K. M. , Jakobsson M., Schmitt T., Tani S, Arndt J. E. (2015). A new digital bathymetric model. *Earth and Space Science*, 331–345.

- Wolf. J., and Woolf. D. (2006). Waves and climate change in the north-east Atlantic. *Geophysical Research Letter*, 33.
- World Meteorological Organization. (1998). *A guide to wave analysis and forecasting*. Geneva: World Meteorological Organization.
- Yasha Hetzel, Ivica Janekovic, Charitha Pattiaratchi ,Wijeratne E.M.S. (2015). Storm surge risk from transitioning tropical cyclones in Australia. *Transitioning tropical cyclones in Australia*. Auckland, New Zealand.